SANDIA REPORT
SAND2010-1635
Unlimited Release
Printed April 2010

MELCOR 1.8.5 Modeling Aspects of Fission Product Release, Transport and Deposition

An Assessment with Recommendations

Randall O. Gauntt

Prepared by
Sandia National Laboratories
Albuquerque, New Mexico 87185 and Livermore, California 94550

Sandia is a multiprogram laboratory operated by Sandia Corporation,
a Lockheed Martin Company, for the United States Department of Energy's
National Nuclear Security Administration under Contract DE-AC04-94AL85000.

Issued by Sandia National Laboratories, operated for the United States Department of Energy by Sandia Corporation.

Available to DOE and DOE contractors from
U.S. Department of Energy
Office of Scientific and Technical Information
P.O. Box 62
Oak Ridge, TN 37831

Telephone: (865) 576-8401
Facsimile: (865) 576-5728
E-Mail : reports@adonis.osti.gov
Online ordering: http://www.osti.gov/bridge

Available to the public from
U.S. Department of Commerce
National Technical Information Service
5285 Port Royal Rd.
Springfield, VA 22161

Telephone : (800) 553-6847
Facsimile : (703) 605-6900
E-Mail : orders@ntis.fedworld.gov
Online order : http://www.ntis.gov/help/ordermethods.asp?loc=7-4-0#online

SAND2010-1635
Unlimited Release
Printed April, 2010

MELCOR 1.8.5 Modeling Aspects of Fission Product Release, Transport and Deposition An Assessment with Recommendations

Randall O. Gauntt
Reactor Modeling and Analysis Department
P.O. Box 5800
Albuquerque, NM, 87185-0736
USA

ABSTRACT

The Phebus and VERCORS data have played an important role in contemporary understanding and modeling of fission product release and transport from damaged light water reactor fuel. The data from these test programs have allowed improvement of MELCOR modeling of release and transport processes for both low enrichment uranium fuel as well as high burnup and mixed oxide (MOX) fuels. This paper discusses the synthesis of these findings in the MELCOR severe accident code.

TABLE OF CONTENTS

LIST OF TABLES

LIST OF FIGURES

1 Fission Product Release and Speciation

The following report presents recommended MELCOR specifications for modeling the release of fission products from reactor fuel under severe accident conditions. The present recommendations modify the default specifications in MELCOR 1.8.5. Separate specifications are provided for use of the models in the analysis of either in-vessel fission product release or spent fuel pool release conditions. In-vessel and spent fuel releases are expected to differ qualitatively due to differences in the reduction/oxidation potentials of steam and air. The motivations for these recommended changes are presented along with an assessment of model predictions using these recommendations against fission product release data from both in-pile and out-of-pile tests.

The current MELCOR default settings for calculating fission product release specify the CORSOR-M release model, described in the MELCOR Reference manuals and in a Battelle report [1]. Also described in these references are the CORSOR and the Booth diffusion release model, implemented in MELCOR as the CORSOR-Booth optional release model. The CORSOR and CORSOR-M models are classified as *fractional release rate* models, differing only slightly in mathematical form, which specify the fractional release rate of the fission product inventory remaining unreleased up to that time. These are empirical models that are based largely on the results of the small-scale, out-of-pile, HI and VI experiments performed at ORNL.

The Booth diffusion model is by comparison a phenomenological model, albeit simplified, that describes the transport of fission products within fuel grains to the grain surface as a diffusion process. In the MELCOR implementation of the Booth diffusion treatment, a gas-phase transport process is added to describe transport of fission products from grain surfaces to the ambient atmosphere. Elements such as molybdenum that are modeled in MELCOR as having very low vapor pressures are ultimately released at low rates regardless of the rate of diffusion within the grain. Once released from the fuel, fission product class combinations can be defined, such as CsI, in order to represent fission product chemistry and speciation. In the present code architecture, multiple combination assignments such as CsI and Cs_2MoO_4 were not foreseen and must be approximated. Once assigned to the chemical class on release, generally, no additional chemistry is allowed. An exception is the treatment of CsI. CsI can chemisorb onto surfaces. Iodine can subsequently revaporize leaving the permanently chemisorbed Cs attached to a surface

Critical assessments of these models and their performance have up to now been few in number, due partly to the lack of additional quality data for comparison to model predictions. One assessment performed by ORNL with MELCOR 1.8.2 surveyed the performance of the MELCOR default models when applied to the VI series of tests [2]. The report observed that while total releases could often be adequately predicted that the release rates were often not in good agreement with the data. Recommendations were provided for code modeling improvements, including provision to vary release based on the H_2/H_2O environment. Recently however, additional experimental data have come available from international testing programs, in particular the French VERCORS

program and the Phebus integral experiments. A recent user assessment of current MELCOR release models in the prediction of these tests has identified some deficiencies that are remedied partly by the recommendations of this report. The Phebus experiments in particular reveal shortcomings of the empirical CORSOR and CORSOR-M models with respect to release rates during the initial fuel heatup, and have been found to significantly overestimate early release rates even though total integral releases might compare reasonably well. Additionally, the integral Phebus tests provide release data under conditions that are significantly less coherent in terms of temperature and oxidation/reduction conditions than in the small scale tests (HI, VI and VERCORS) where the fuel samples are small, temperatures are uniform and oxidation/reduction conditions controlled and constant. The Phebus experiments provide conditions for release that are more representative of conditions expected in the full-scale reactor accident case, and are used as the principal basis for judging the performance of the MELCOR release models.

2 MELCOR Release Models

The release rate models in MELCOR are briefly summarized as follows. The original CORSOR model correlates the *fractional* release rate coefficient in exponential form,

$$k = A\ \exp(B\,T) \qquad for\ T \geq T_i \qquad \text{Eq. 1}$$

where k is the release rate (fraction per minute), *A* and *B* are empirical coefficients based on experimental data, and *T* is the core cell component temperature in degrees Kelvin. Different values for *A* and *B* are specified for three separate temperature ranges. The lower temperature limit T_i for each temperature range and the *A* and *B* values for that range are defined for each class in sensitivity coefficient in array 7101 of the MELCOR computer code. If the cell temperature is calculated to be below the lowest temperature limit specified, no release is calculated.

2.1 CORSOR-M

The CORSOR-M model correlates the same release data used for the CORSOR model using an Arrhenius form,

$$k = k_o \exp(-Q/RT) \qquad \text{Eq. 2}$$

The values of k_o, Q, and T are in units of min^{-1}, kcal/mole, and K, respectively. The value of R is 1.987 x 10^{-3} in (kcal/mole)K^{-1}. The values of k_o and Q for each class are implemented in sensitivity coefficient array 7102 in the MELCOR computer code.

2.2 CORSOR-Booth

The CORSOR-Booth model considers mass transport limitations to radionuclide releases and uses the Booth model for diffusion with empirical diffusion coefficients for cesium releases. Release fractions for other radionuclide classes are calculated relative to that for cesium. The effective diffusion coefficient for cesium in the fuel matrix is given by

$$D = D_o \exp(-Q/RT) \qquad \text{Eq. 3}$$

where R is the universal gas constant, T is the temperature, Q is an activation energy, and the pre-exponential factor D_0 is a function of the fuel burn-up. The cesium release fraction, *f*, at time t is calculated from an approximate solution of the diffusion equation for fuel grains of spherical geometry [3],

$$f = 6\ \sqrt{\frac{D' t}{\pi}} - 3\ D' t \qquad \text{for } D' t\ < 1/\pi^2 \qquad \text{Eq. 4}$$

$$f = 1 - \frac{6}{\pi^2} \exp(-\pi^2 D' t) \qquad \text{for } D' t > 1/\pi^2 \qquad \text{Eq. 5}$$

where

$D' t$ = $D t / a^2$ (dimensionless), and

a = equivalent sphere radius for the fuel grain

The release rate of Cs during a time interval t to t+Δt from the fuel grain is calculated as

$$\text{Release rate}_{Cs} = \frac{\left[f\left(\sum D' \Delta t\right)_{t+\Delta t} - f\left(\sum D' \Delta t\right)_t \right] V \rho}{F \Delta t} \qquad \text{Eq. 6}$$

where ρ is the molar density in the fuel, V is the fuel volume, F is the fraction of the Cs inventory remaining in the fuel grain, and the summations are done over the timesteps up to time $(t + \Delta t)$ and t, respectively.

The release rate formulation in the CORSOR-Booth model is also limited by mass transfer through the gas-phase. The gas-phase mass transport release rate from the fuel rod for species k, $\dot{m}_k$, is calculated using an analogy from heat transfer as

$$\dot{m}_k = \left[\frac{A_{fuel} Nu\, D_{k,gas}}{D_{fuel} RT} \right] \cdot \left(P_{k,eq} - 0 \right) \qquad \text{Eq. 7}$$

where

D_{fuel} = diameter of fuel pellet
A_{fuel} = fuel rod flow contact area
$D_{k,gas}$ = diffusivity of class k in the gas mixture
Nu = Nusselt number
$P_{k,eq}$ = equilibrium vapor pressure of class k at temperature T.

In the mass transfer term, the driving potential is the difference in partial pressure at the surface of the grain and the pressure in the free stream atmosphere. Here, the free stream partial pressure is assumed to be approximately zero.

The effective release rate for Cs given by Equation 6 is a combination of the rates given by diffusion and by gas-phase mass transport. Therefore, the contribution from diffusion only is taken as

$$DIFF_{Cs} = \left[\frac{1}{\text{Release rate}_{Cs}} - \frac{1}{\dot{m}_{Cs}} \right]^{-1} \qquad \text{Eq. 8}$$

The diffusion release rate for species other than cesium is given by multiplying the cesium release rate by an appropriate scaling factor S_k for each radionuclide class k:

$$DIFF_k = DIFF_{Cs} S_k \qquad \text{Eq. 9}$$

The combined mass transport and diffusion release rate $\dot{m}_{tot,k}$ for radionuclide class k is then

$$\dot{m}_{tot,k} = \frac{1}{DIFF_k^{-1} + \dot{m}_k^{-1}} \qquad \text{Eq. 10}$$

Inspection of equations 10 together with equation 7 reveals that the release predicted by the MELCOR models can be mass transfer limited by low vapor pressures even if the diffusive transport is large.

2.3 Known Limitations of MELCOR Release Models

The fission product release models implemented in MELCOR are quite simplified and are more than a decade old. The implemented models base the release of all radionuclide chemical classes on the release predicted for Cs, which in the Booth model is appropriately considered a diffusion process. Scaling factors are used to estimate release of other species based on the fit to experimentally observed Cs release in spite of the fact that it is recognized that likely not all fission product classes diffuse at the same rate out of the fuel grains, nor are all principal release mechanisms well represented as a diffusion process. Consideration of speciation in MELCOR release models is simplified and for the most part fixed at the time of release to represent the predominating speciation. The vapor pressures of the MELCOR release classes are defined to represent the presumed fission product speciation.

A better treatment would be to allow the vapor pressure to be adjusted to account for local speciation affected by oxidizing or reducing conditions and to then source these species into appropriate chemical classes. Such modifications are probably needed for Te, Ba, Mo, UO_2 and Ru. Provision does exist to consider the extent of cladding oxidation to attempt to simulate retention of Te or Ba, but data are needed to use this provision effectively. Separate diffusion coefficients for each of the volatile classes would probably be appropriate, and a UO_2 oxidation model is needed to account for the effect of stoichiometry on diffusion and to predict fuel volatilization. UO_2 volatilization may be responsible for release of UO_3 as well as other less volatile species because of physical stripping of the fuel matrix containing the fission products. A number of more recently evolved release models consider the effect of fuel stoichiometry on the diffusion coefficient as well as the oxidizing/reducing potential of the environment [4,5,6,7]. The VICTORIA code considers a very large number of potential fission product species in a thermodynamic equilibrium approach. Some simplifications to this potentially numerically burdensome approach may be needed [8].

In the more recent models, fission products are classified often into three main groups, volatile (Xe, Cs, I, Te) semi-volatile (Ru, Ba, La, Ce) and non-volatile (UO_2 and actinides). Volatile fission products are released based on the Booth diffusion model where the diffusion coefficient includes effects of UO_2 hyper-stoichiometry. The hyper-stoichiometry, in turn, is determined by a fuel oxidation model. Releases of semi-volatile fission products are strongly affected by vapor pressure which in turn is affected by speciation determined by the oxidizing/reducing conditions that arise as steam, air and hydrogen interact with zirconium alloy cladding at the location. Non-volatile release may be dominated by UO_2 volatilization by formation of UO_3, producing fuel matrix degradation and fuel vaporization. The French Elsa code follows this approach, using models similar to those reported by Lewis et al. [4,5].

More detailed (and flexible) release modeling can be adopted in MELCOR in the future. The importance of accounting for speciation and the ensuing effect on species volatility (vapor pressure) is clear. In the present approach, as described in the next section of this report, assumptions are made about the dominant speciation at the time of release and maintaining this assumed speciation globally throughout the core region. A more elegant model would allow variation of release speciation as conditions in the core change locally and temporally with respect to steam and hydrogen concentrations. In the case of air exposure, such as in spent fuel pool accidents, different assumptions about speciation, especially concerning Ru release, are needed. [9]

3 Assessment of MELCOR Default Release Models

Whereas the HI-VI ORNL tests provided the original basis for development of the MELCOR fission product release models, the Phebus FPT-1 integral experiment is used as the principal basis for evaluation of release modeling options. In previous assessment exercises, in particular the ISP-46 (International Standard Problem 46 [10]), the MELCOR default CORSOR-M release model was found to predict reasonably total release fractions for many fission products. On the other hand, the empirical model was found by many MELCOR ISP participants to over predict the initial release rates. Similar, rapid, early release is also found for the CORSOR option. The Booth diffusion treatment for release is thought to be a superior model since it has some basis on a physical transport process. However, investigation of the MELCOR CORSOR-Booth option using the default Booth release parameters was found to produce inferior results, with total release of Cs and other fission products being significantly underpredicted in test FPT-1. In view of this, a review of the literature was undertaken and revealed numerous, more recent, parameter-fits to the Booth solution.

3.1 Proposed Modifications to MELCOR Booth Release Modeling

A number of these alternative models are described in an ORNL report that recommends updated values for the previously discussed models [11]. Shown in Figure 1 are release fractions predicted at a constant temperature of 2000K by the various release models discussed in the ORNL report. It can be seen that fractional release rate model, CORSOR-M, predicts the largest release rate of all of the models. This trend is consistent with observations from analyses considering measured releases from FPT-1. Similarly, the CORSOR-Booth diffusion model predicts the lowest release rate of all of the models. This too is consistent with MELCOR analyses of FPT-1 using these modeling parameters. Judging that a best fit might lie somewhere in between these extremes, the ORNL-Booth parameters were investigated in MELCOR analyses of FPT-1, wherein significantly improved release predictions were obtained. The ORNL-Booth parameters were recommended over the CORSOR-Booth parameters in the 1995 ORNL report. The ORNL-Booth model is specified by the parameters in Table 1. Figure 2 shows other comparisons between the ORNL-Booth and CORSOR-M release behaviors. The fractional release rates for the two models obtained by differentiating the release fractions in Figure 2 are shown in Figure 3.

Table 1. CORSOR-Booth, ORNL-Booth and Modified ORNL-Booth Parameters

	CORSOR-Booth	ORNL-Booth	Adjusted ORNL-Booth
Diffusion coeff. D_o	2.5×10^{-7} m^2/sec	1×10^{-6} m^2/sec	1×10^{-6} m^2/sec
Activation Energy Q	3.814×10^5 Joule/mole	3.814×10^5 Joule/mole	3.814×10^5 Joule/mole
Grain radius, a	6 μm	6 μm	6 μm
Class Scale Factors	---	---	---
Class 1 (Xe)	1	1	1
Class 2 (Cs)	1	1	1
Class 3 (Ba)	3.3×10^{-3}	4×10^{-4}	4×10^{-4}
Class 4 (I)	1	0.64	0.64
Class 5 (Te)	1	0.64	0.64
Class 6 (Ru)	1×10^{-4}	4×10^{-4}	0.0025
Class 7 (Mo)	0.001	0.0625	0.2
Class 8 (Ce)	3.34×10^{-5}	4×10^{-8}	4×10^{-8}
Class 9 (La)	1×10^{-4}	4×10^{-8}	4×10^{-8}
Class 10 (U)	1×10^{-4}	3.6×10^{-7}	3.2×10^{-4}
Class 11 (Cd)	0.05	0.25	.25
Class 12 (Sn)	0.05	0.16	.16

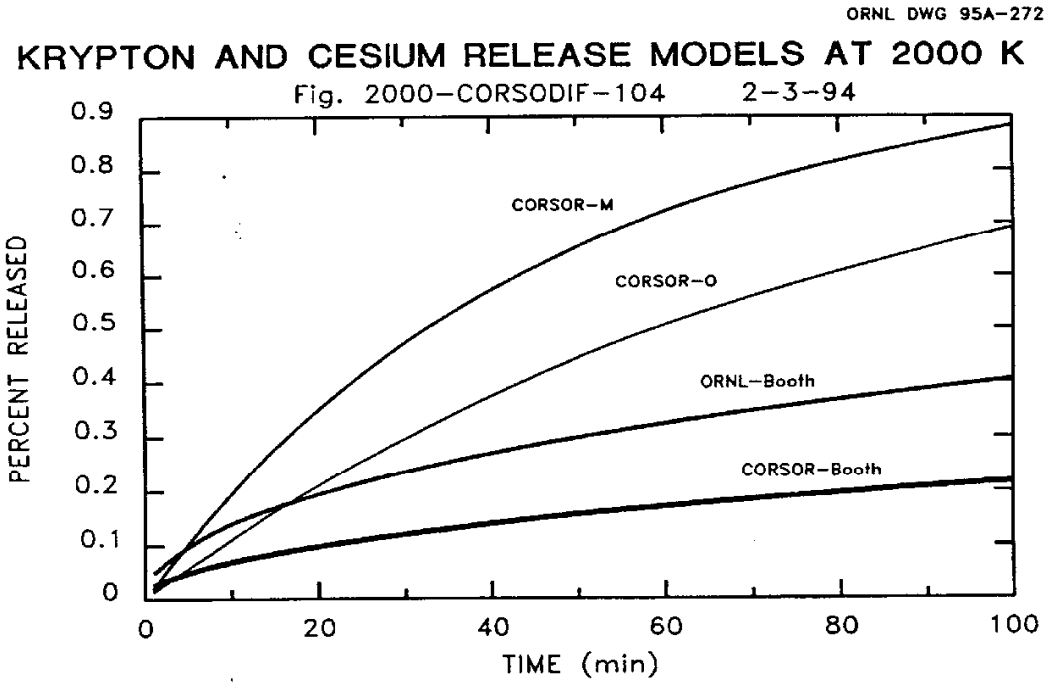

Figure 1. Release fractions for different release models – release temperature 2000K. Note CORSOR-M produces largest release whereas CORSOR-Booth produces the smallest release.

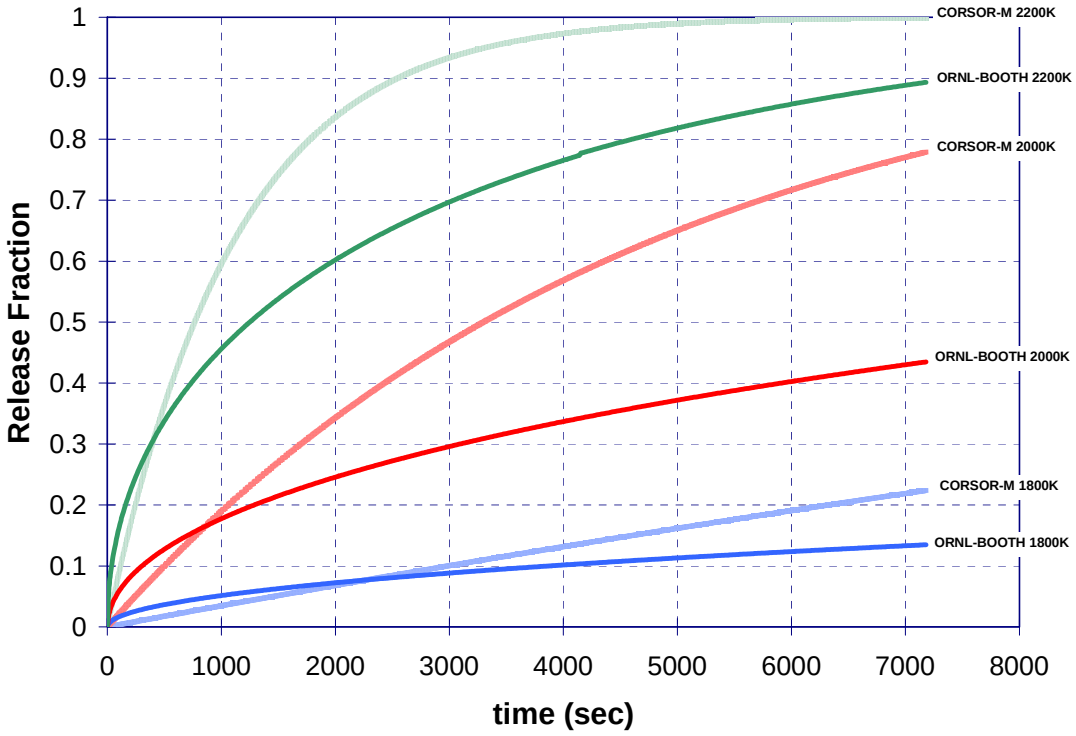

Figure 2. Release fractions at constant temperature for ORNL-Booth versus CORSOR-M.

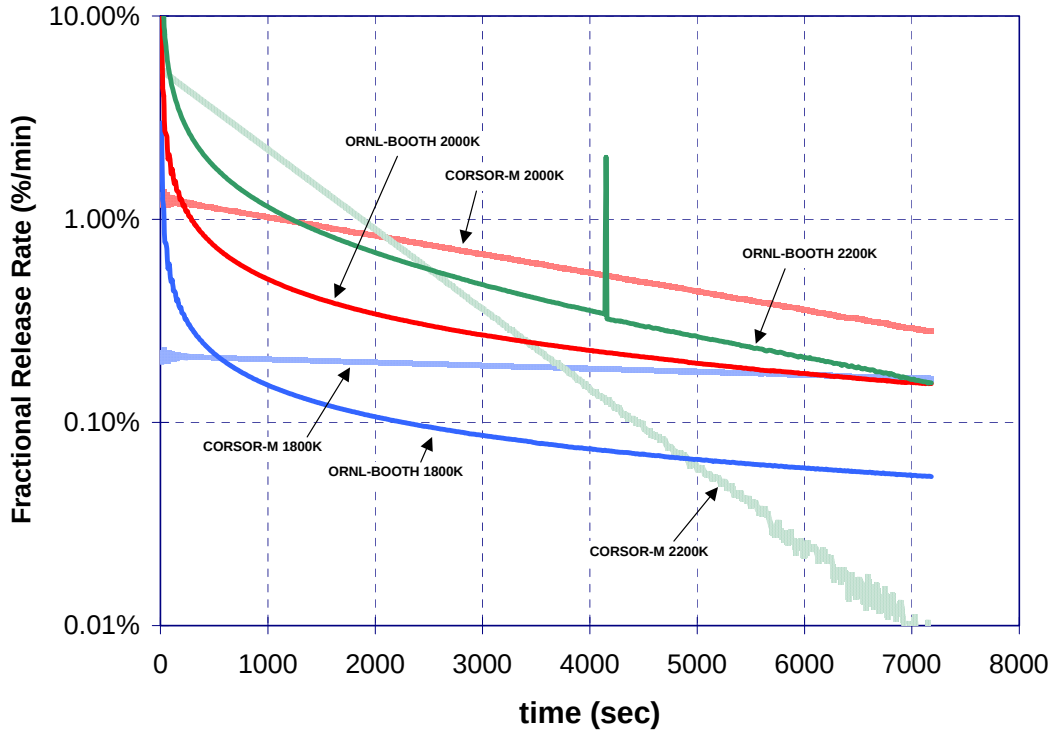

Figure 3. Fractional release rate (%/min) - the time derivative of the release fraction.

While significant improvements in release behavior were obtained for the analysis of the FPT-1 test with the as-reported ORNL-Booth parameters, some additional modification to the MELCOR release model was pursued. Evidence from the Phebus experiments indicates that the dominant chemical form of released Cs is cesium molybdate - Cs_2MoO_4. This is based on deposition patterns in the Phebus experiment where Cs is judged to be in aerosol form at 700C, explaining deposits in the hot upper plenum of the Phebus test section, and deposition patterns in the cooler steam generator tubes. In recognition of this, the vapor pressure of both Cs and Mo classes were defined to be that of Cs_2MoO_4. While having little effect on the net release of Cs, this change had a significant effect on the release of Mo. The MELCOR default options have an exceedingly low Mo vapor pressure. The net release is limited by the vapor transport term, as expressed in Eq. 7 and Eq. 8. Vapor pressures for selected fission product species are shown in Figure 4. Defining the Mo vapor pressure to be that of Cs_2MoO_4 produced significantly improved predictions of Mo release rates with respect to observed FPT-1 releases, as will be discussed in the next section of this report.

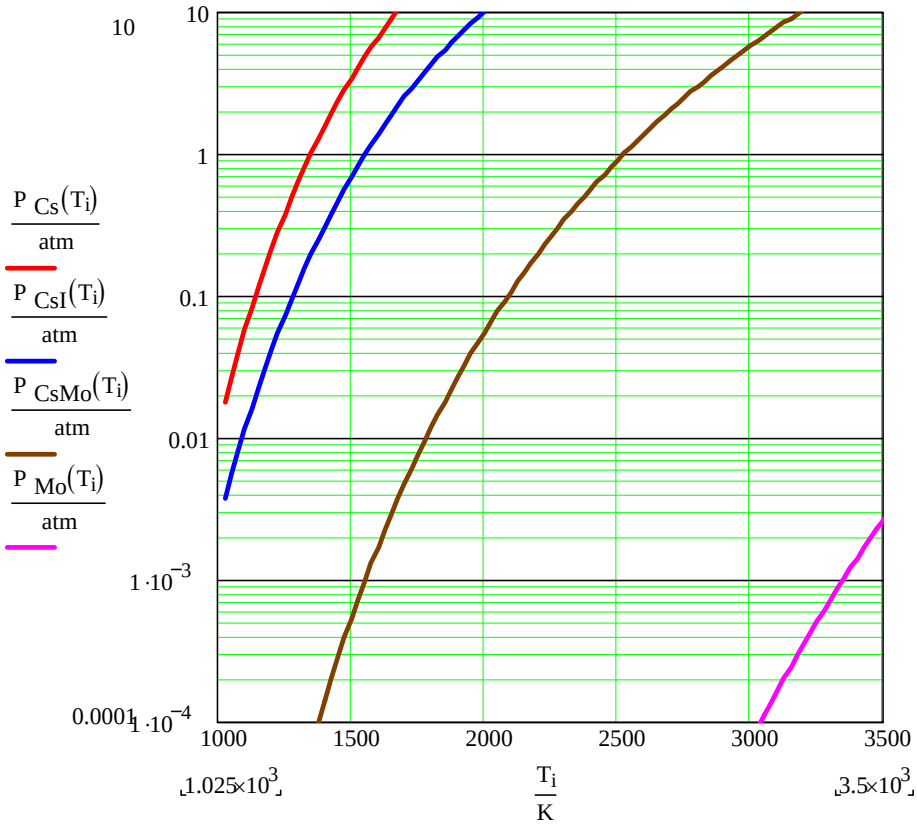

Figure 4. Vapor pressures of selected species.

3.2 Assessment of Modified ORNL-Booth Model Against Phebus FPT-1

The Phebus program provides the best source of prototypic data on fission product release from irradiated fuel. The Phebus experiments have benefitted from many lessons learned from earlier, similar, experimental efforts and from advances in testing technology, instrumentation, etc. A schematic of the Phebus test facility is shown in Figure 5. A previously irradiated fuel bundle of about a meter in length is situated in the irradiation cavity in the Phebus test reactor. The fuel bundle is re-irradiated within the reactor to build up the inventories of short lived fission products such as isotopes of iodine. Then, this fuel bundle is subjected to severe damage from nuclear heating and oxidation by injected steam. Fission products released from the test bundle flow through a heated section representing the reactor coolant system (RCS), through a simulated steam generator tube where extensive deposition can occur, and into a simulated containment where fission product fallout occurs.

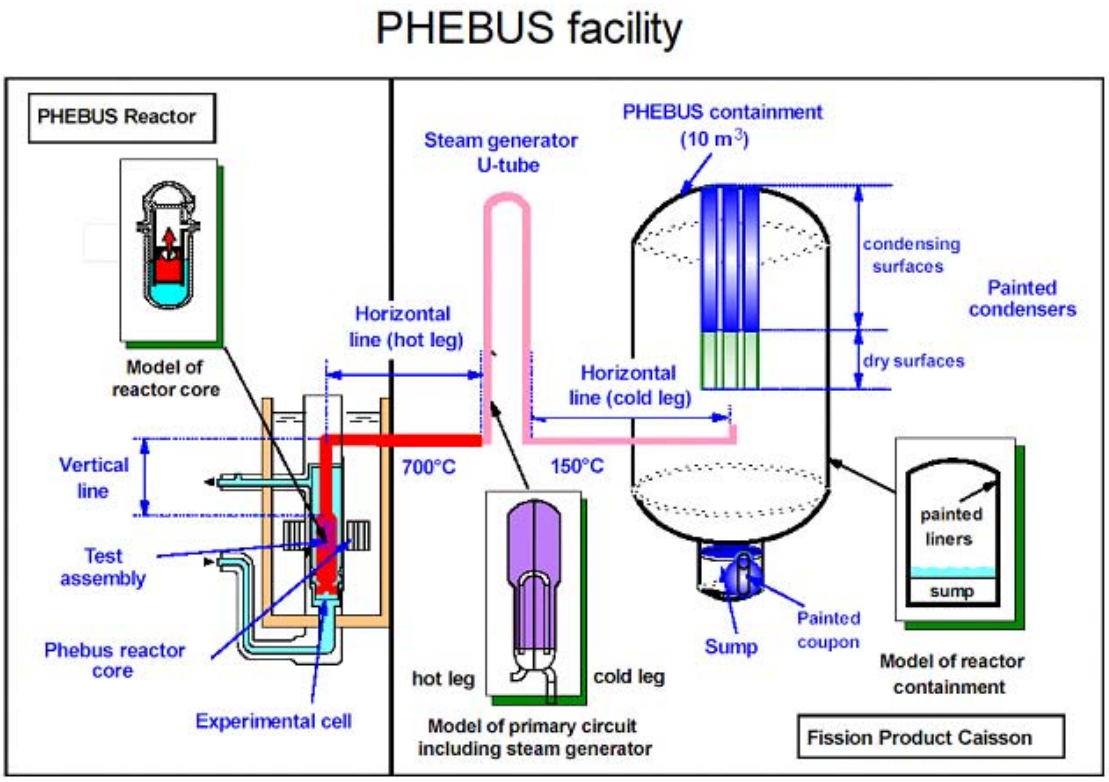

Figure 5. Schematic of the Phebus test facility showing test fuel bundle, heated lines, steam generator tube and simulated containment.

Shown in Figure 6 is the nuclear heating history that was used in test FPT-1 to heat the bundle to simulate severe accident decay heating conditions. The chemical heating produced by steam-Zr oxidation is also shown in the figure. The temperature response of the test fuel is shown in Figure 7 where the temperature transient caused by the additional oxidation heating is clearly evident. During this time, fission products are also released where oxidation conditions vary from oxidizing to reducing, depending on elevation in the test bundle. Figure 8 shows the end state of the test bundle at the conclusion of the experiment.

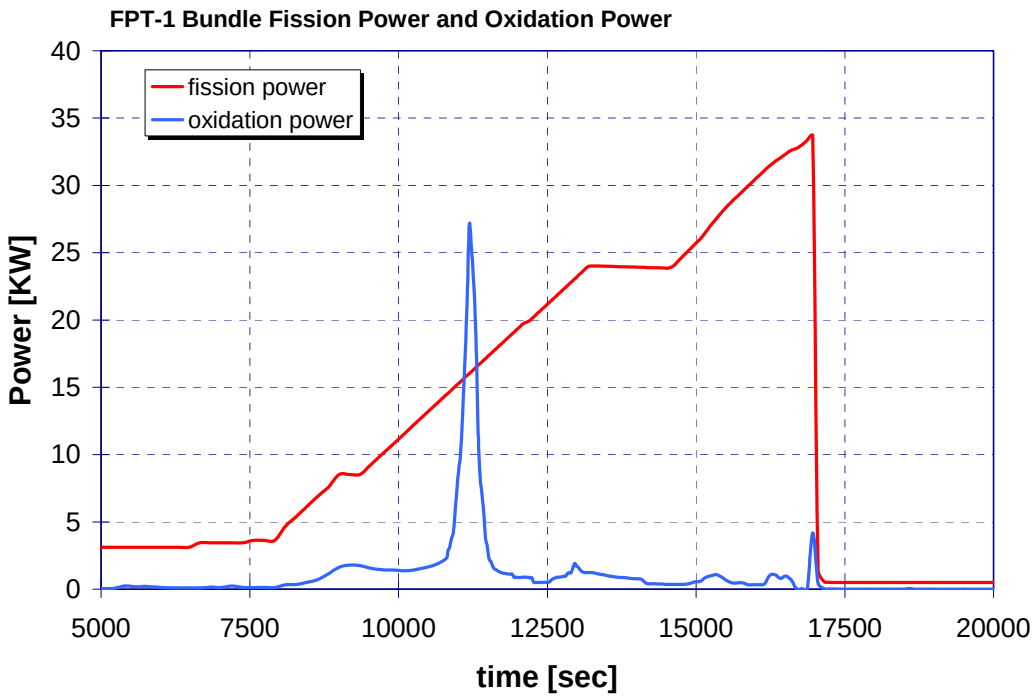

Figure 6. FPT-1 Nuclear and chemical heating history.

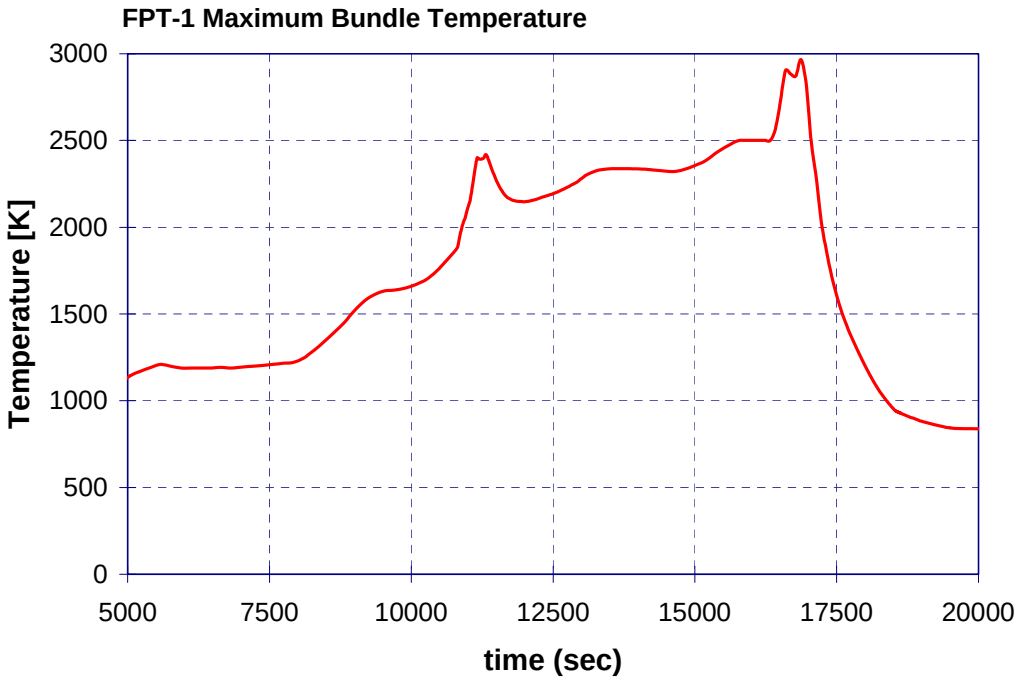

Figure 7. FPT-1 maximum bundle temperature history.

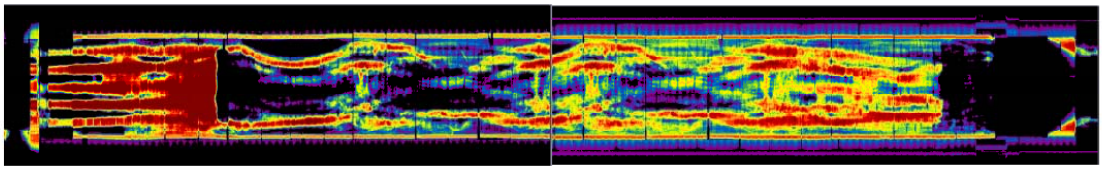

Figure 8. Emission gamma tomography of the end state condition of test FPT-1.

Figure 9 through 20 show the results of using the modified ORNL-Booth model for fission product release in the FPT-1 analysis. Where available, Phebus data are presented in the figures. In most cases, significant improvement is realized in both the early time release time as well as for total predicted release. The release for the Barium class predicted by the ORNL-Booth model is low relative to the data, whereas the release predicted using the CORSOR-M model is high. Improvement to this observed release proved illusive and it is believed that some adjustments to the vapor pressure of Ba to account for some not yet understood barium speciation could produce some improvement. Adjustments to both vapor pressure and scaling factors were rationalized for Mo release based on Phebus program findings, producing good agreement with experiment. The Ru vapor pressure was increased by a factor of 10 to account for some greater volatility attributed to formation of oxides under moderately oxidizing conditions, and the Booth scaling factor was adjusted to obtain agreement with experimental observations. The Booth scaling factor for UO_2 was increased significantly in order to obtain agreement with test observations. This also is rationalized as due to effects of fuel oxidation and greater volatility of fuel oxides. Ce and La release parameters were not adjusted owing to lack of experimental basis, however, it could be reasoned that their releases ought to roughly follow UO_2 release if fuel matrix stripping occurs.

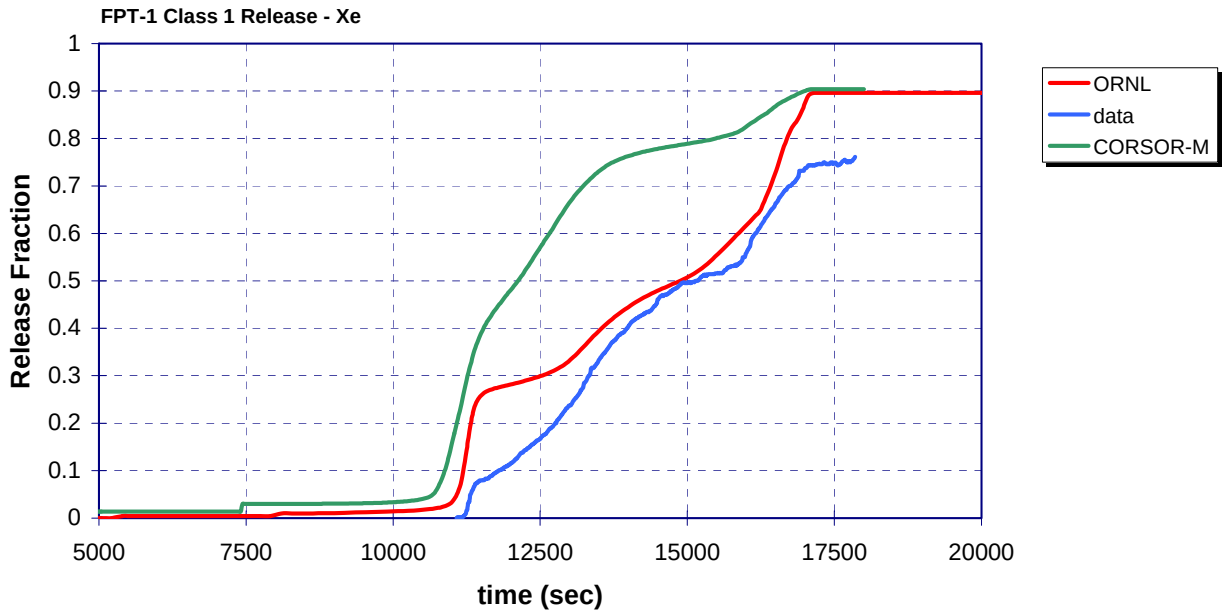

Figure 9. Comparison of ORNL-Booth versus CORSOR-M for Xe release (Class 1)

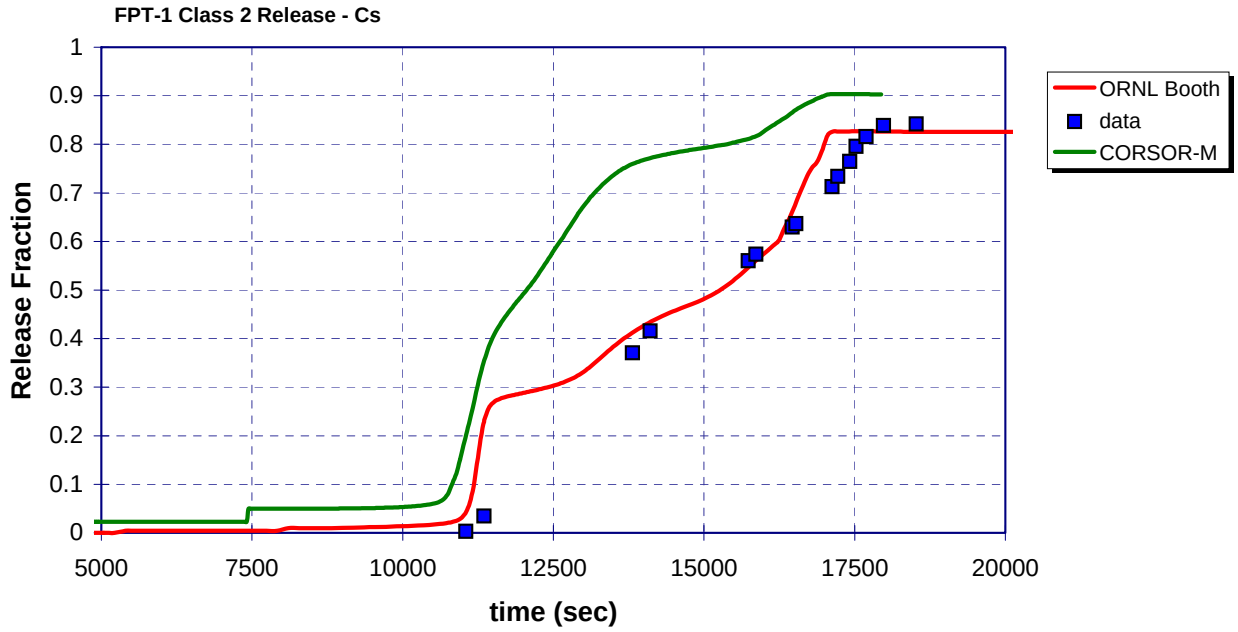

Figure 10. Comparison of ORNL-Booth versus CORSOR-M for Cs release (Class 2).

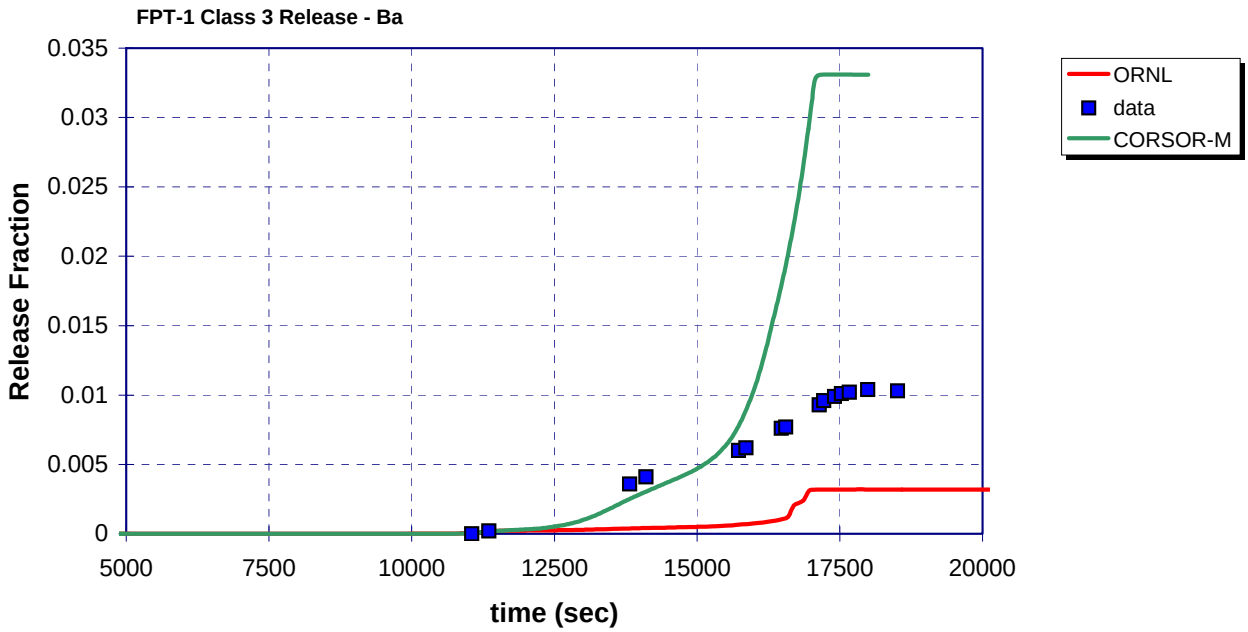

Figure 11. Comparison of ORNL-Booth versus CORSOR-M for Ba release (Class 3).

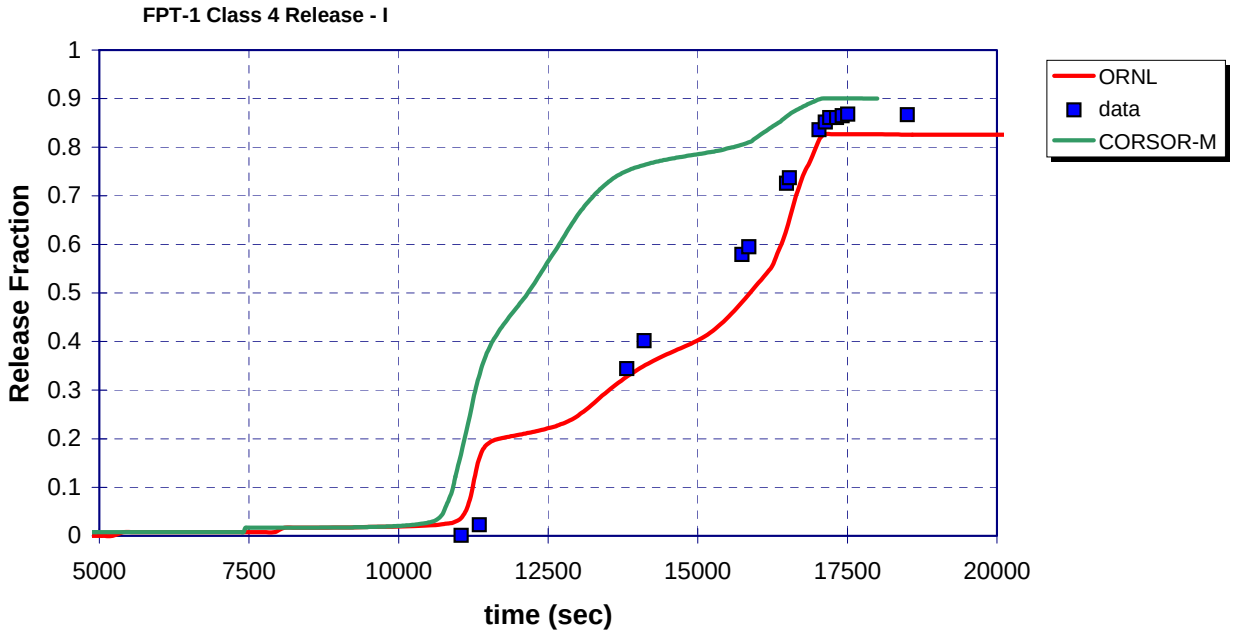

Figure 12. Comparison of ORNL-Booth versus CORSOR-M for I release (Class 4).

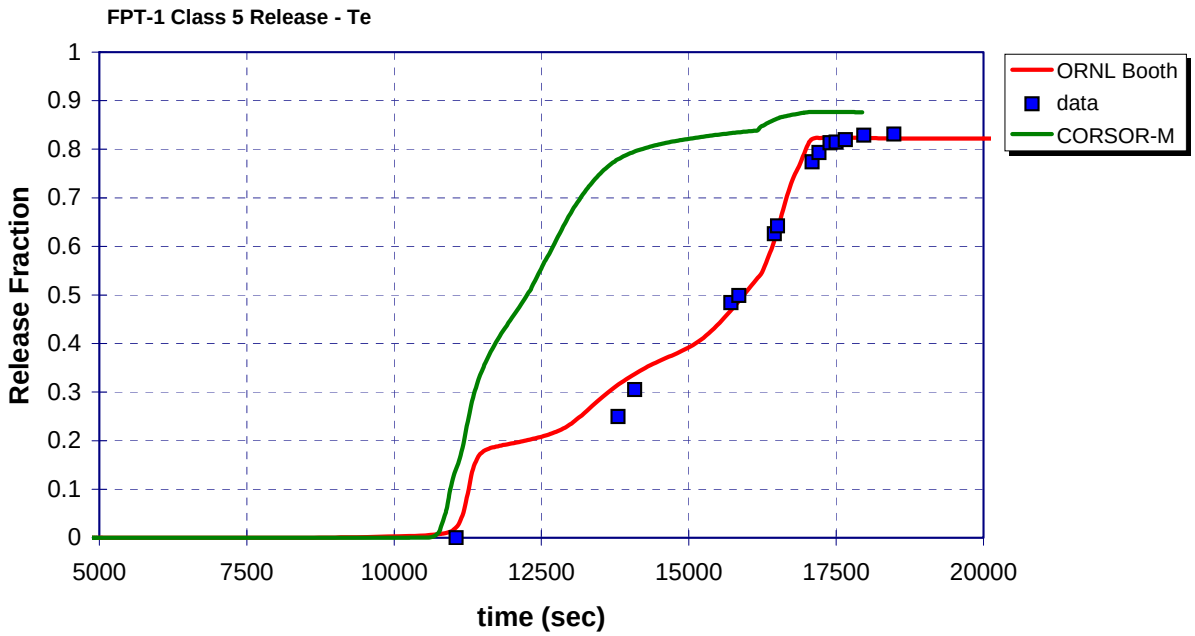

Figure 13. Comparison of ORNL-Booth versus CORSOR-M for Te release (Class 5)

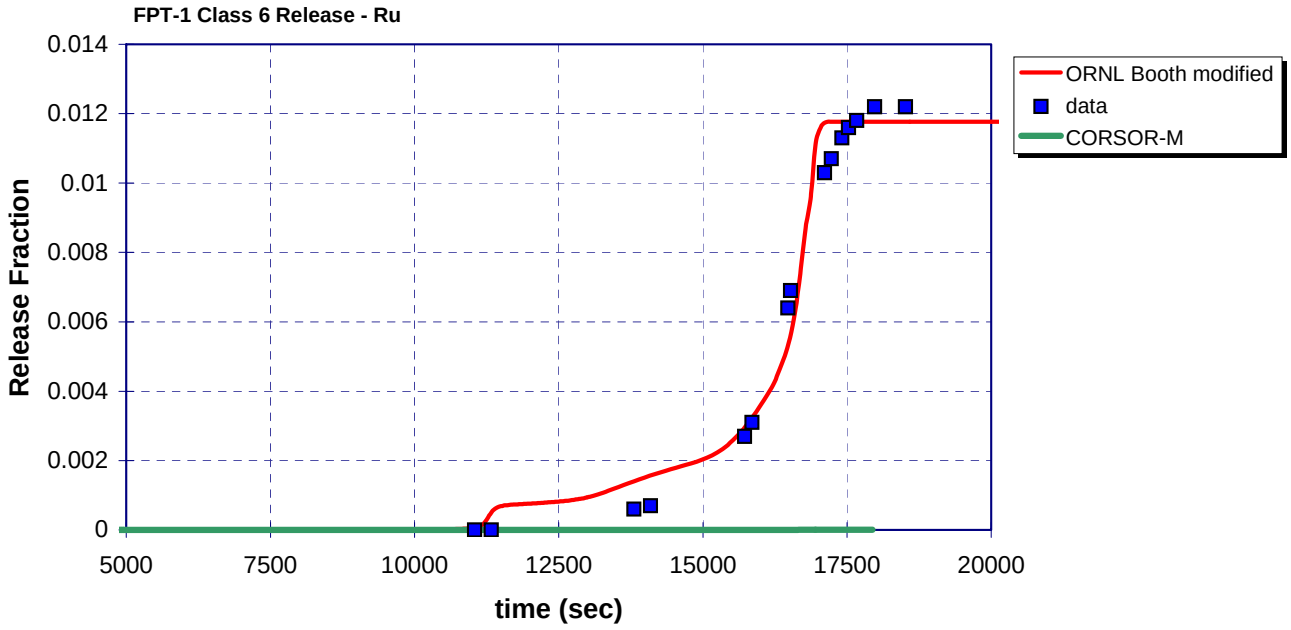

Figure 14. Comparison of ORNL-Booth versus CORSOR-M for Ru release (Class 6)

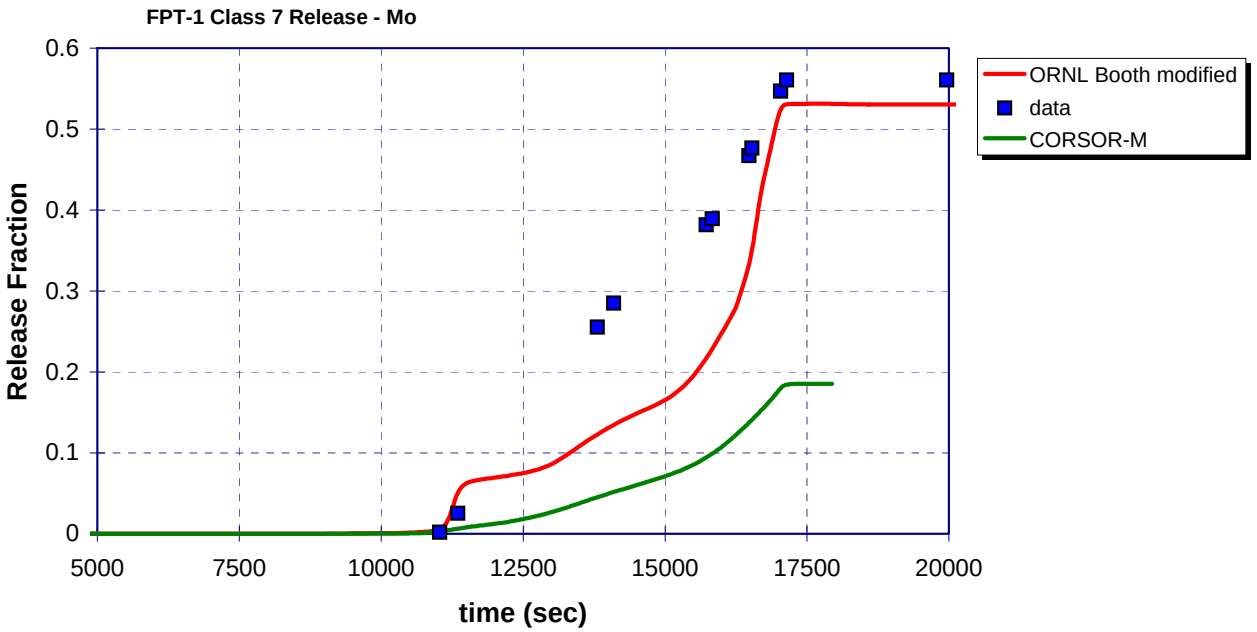

Figure 15. Comparison of ORNL-Booth versus CORSOR-M for Mo release (Class 7). *The Mo vapor pressure was set to correspond to Cs_2MoO_4.*

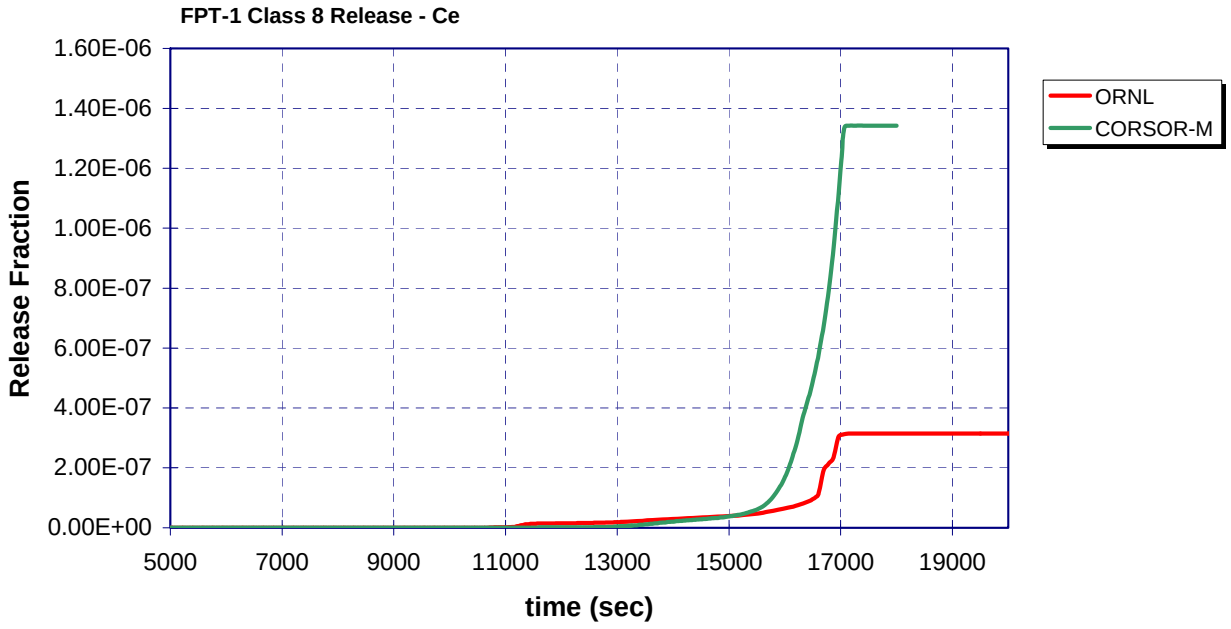

Figure 16. Comparison of ORNL-Booth versus CORSOR-M for Ce release (Class 8).

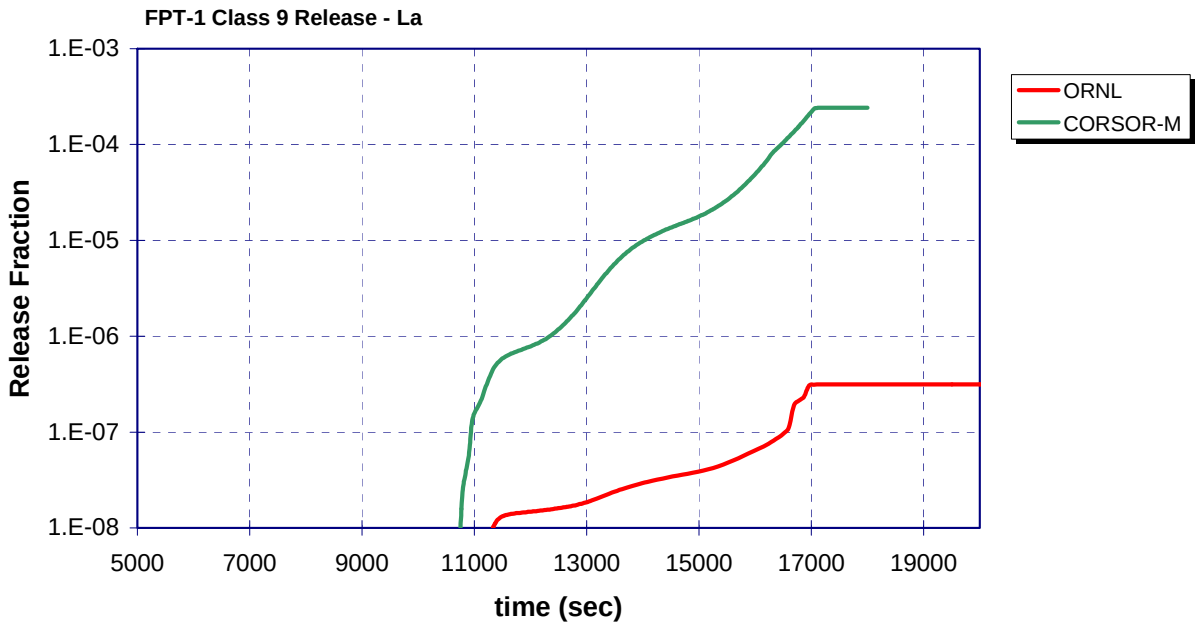

Figure 17. Comparison of ORNL-Booth versus CORSOR-M for La release (Class 9).

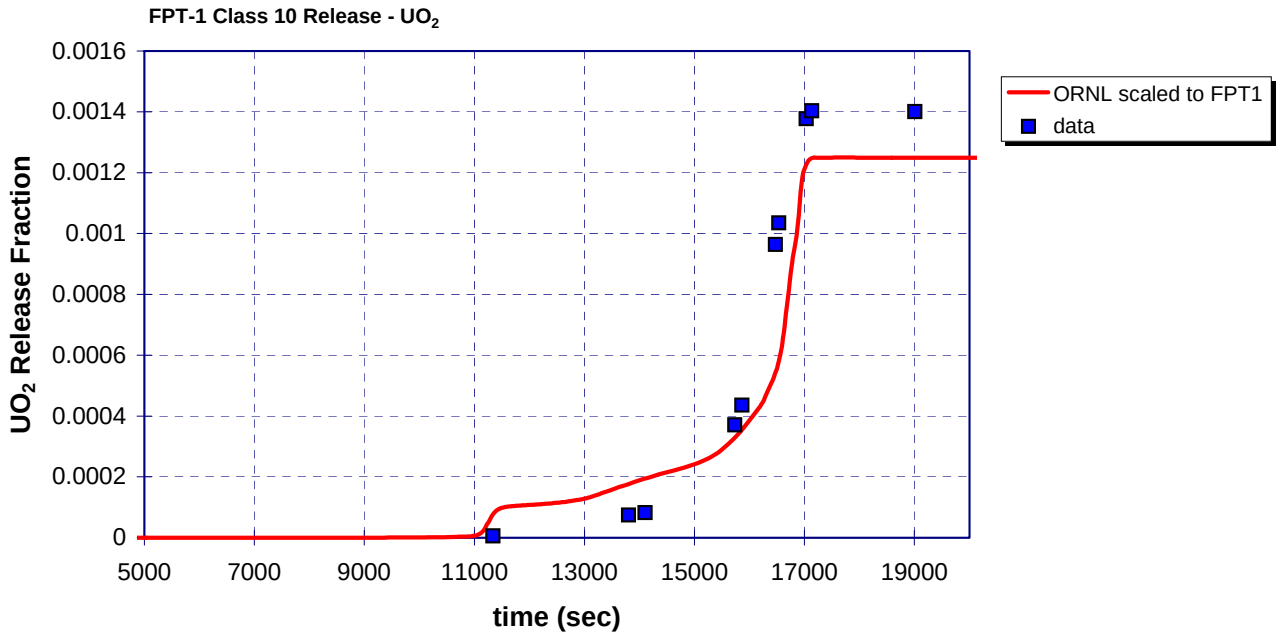

Figure 18. Comparison of ORNL-Booth versus CORSOR-M for UO_2 release (Class 10). *The UO_2 scaling factor was adjusted to match observed releases. La and Ce releases are not expected to be greater than UO_2 release, but may be less owing to lower volatility.*

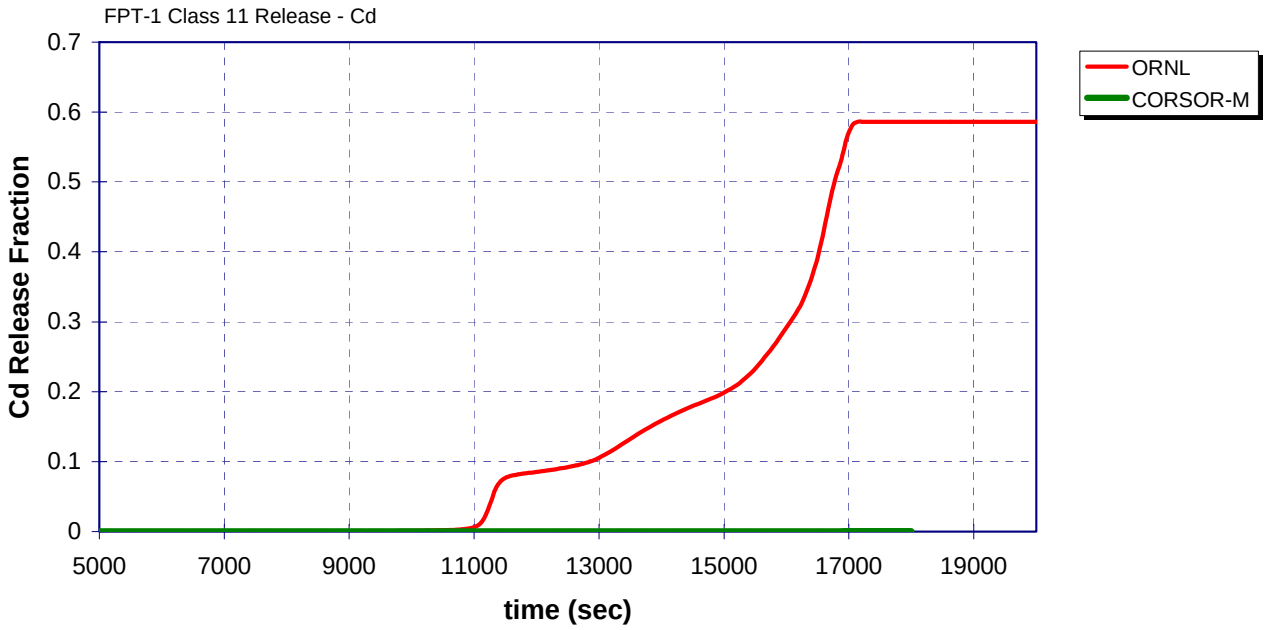

Figure 19. Comparison of ORNL-Booth versus CORSOR-M for Cd release (Class 11).

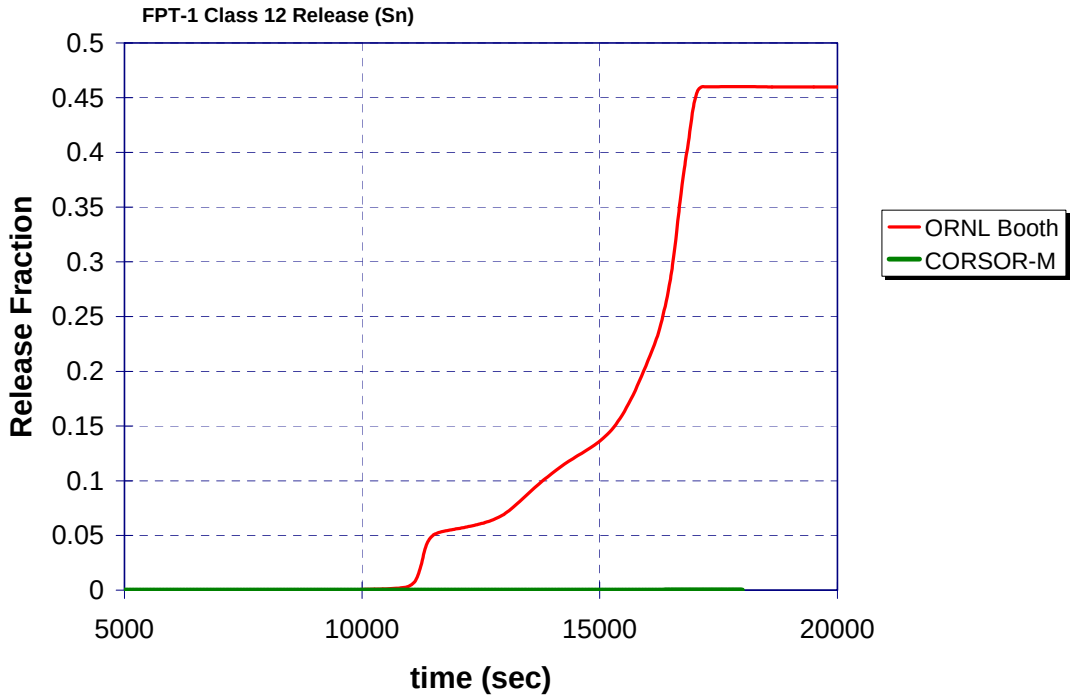

Figure 20. Comparison of ORNL-Booth versus CORSOR-M for Sn release (Class 12).

3.3 Comparison to ORNL VI Tests and VERCOR Tests [12]

After optimizing the ORNL-Booth fission product release parameters for the FPT-1 experiment, it is of interest to compare the modified model to the original ORNL test data upon which the CORSOR-M model was developed. The following section explores the application of the modified ORNL-Booth release modeling to selected ORNL-VI test results and the more recent VERCORS test data. The comparisons are made mainly to the Cs release observed in these experiments since all other releases are simply scaled to the Cs release in the Booth implementation in MELCOR, and these data were readily available. In the case of VERCORS 4, data on release of other fission products were available and comparisons to these releases were made. The MELCOR models were obtained from a recent IBRAE MELCOR Validation exercise [9] investigating the MELCOR default release models. The experimental data were taken from reference [9]. These analyses were performed using a simple MELCOR model of the experiments. The present analyses make use of the modified ORNL-coefficients and compare results with the MELCOR default CORSOR-M release model.

A schematic of the VERCORS testing facility is shown in Figure 21, the general layout is similar in the ORNL VI tests. The tests examined are summarized in Table 2. The tests involved both oxidizing and reducing conditions.

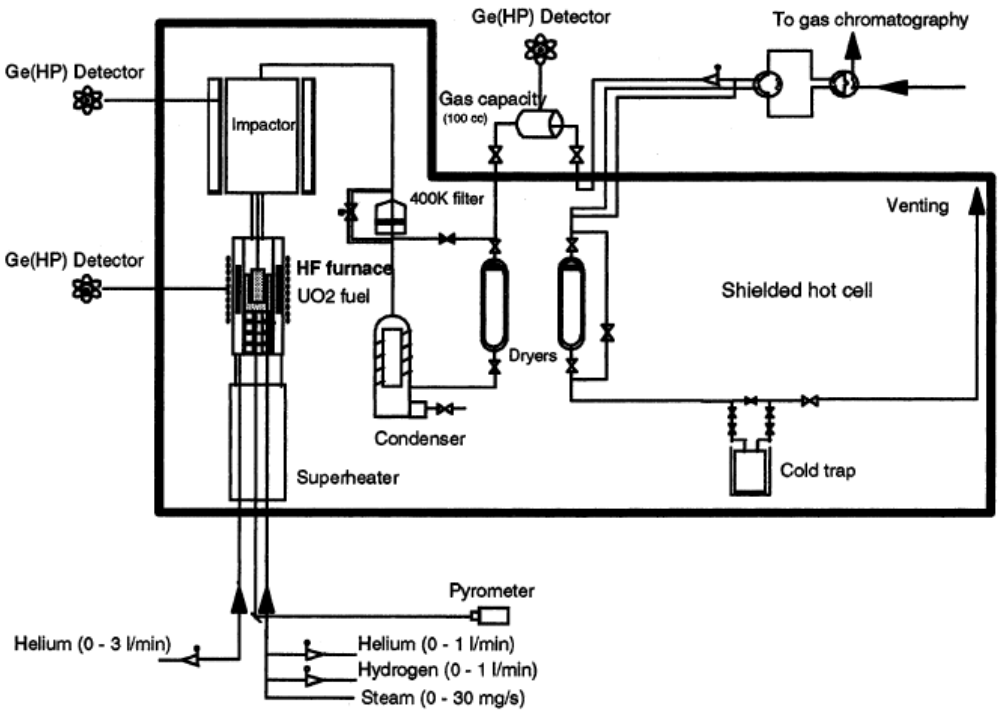

Figure 21. Schematic of VERCORS test facility for measuring fission product release from small fuel samples.

Table 2. Test conditions for selected ORNL VI tests and VERCORS tests.

Test	Hydrogen	Steam	Max Temperature
ORNL VI-2	0	1.8 liter/min	2300K
ORNL VI-3	0	1.6 liter/min	2700K
ORNL VI-5	0.4 liter/min	0	2740K
VERCORS 2	0.027 gm/min	1.5 gm/min	2150K
VERCORS 4	0.012 gm/min	1.5 – 0 gm/min	2573K

In almost all cases, the modified ORNL-Booth model produces improved predictions of the test data, as shown in Figure 22 through Figure 24 for the VI tests, and in Figure 25 through Figure 31 for the VERCORS tests.

In test VI-2 run under steam-rich conditions the peak temperature attained was ~2300K. Both models overpredicted the Cs release for this test, with the modified ORNL-Booth treatment performing slightly better (Figure 22). Test VI-3 was similar to VI-2 except that higher temperatures were attained. In analyses of this test, both models yielded predictions closer to the data. Again the modified ORNL-Booth model performed somewhat better (Figure 23). From these two tests, it appears that release rate in the 2300K range is still slightly over-predicted for oxidizing conditions. Test VI-5 conducted under reducing conditions was well predicted by both models, as shown in Figure 24. Table 3 through Table 5 provides total releases predicted by CORSOR-M and ORNL-Booth compared with totals reported for the ORNL VI tests 2, 3 and 5.

Both VERCORS 2 and 5 were run in mixed conditions with both steam and hydrogen. In VERCORS 5, the steam flow was reduced to zero for the high temperature plateau. During the period of zero flow, the fuel was exposed to reducing conditions since the ambient atmosphere contained little steam and much hydrogen. Test VERCORS 2, like ORNL-VI2 was performed at a lower temperature and produced a comparatively lower Cs release (Figure 25). The modified ORNL-Booth model captured this lower release where the CORSOR-M model did not. Test VERCORS 4 was performed under completely reducing conditions during the release phase. In this case CORSOR-M underpredicted release, whereas the modified ORNL-Booth model captured the release behavior reasonably well.

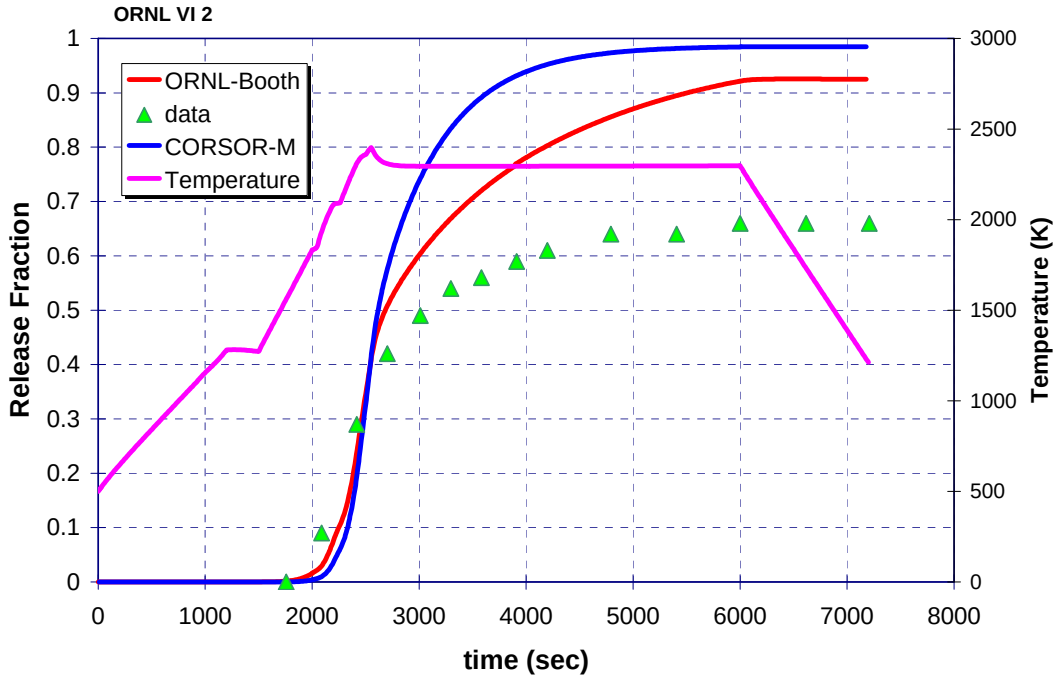

Figure 22. Comparison of Cs release for ORNL Booth modified with CORSOR-M for VI-2 run under steam oxidizing conditions.

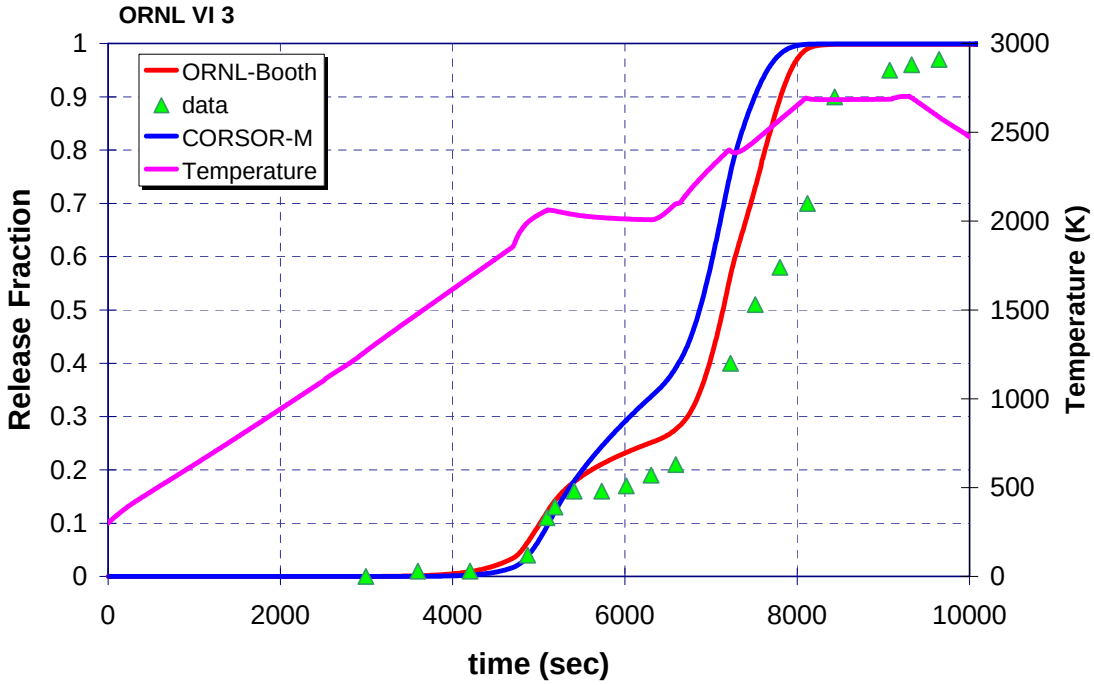

Figure 23. Comparison of Cs release for ORNL Booth modified with CORSOR-M for VI-3 performed under steam oxidizing conditions.

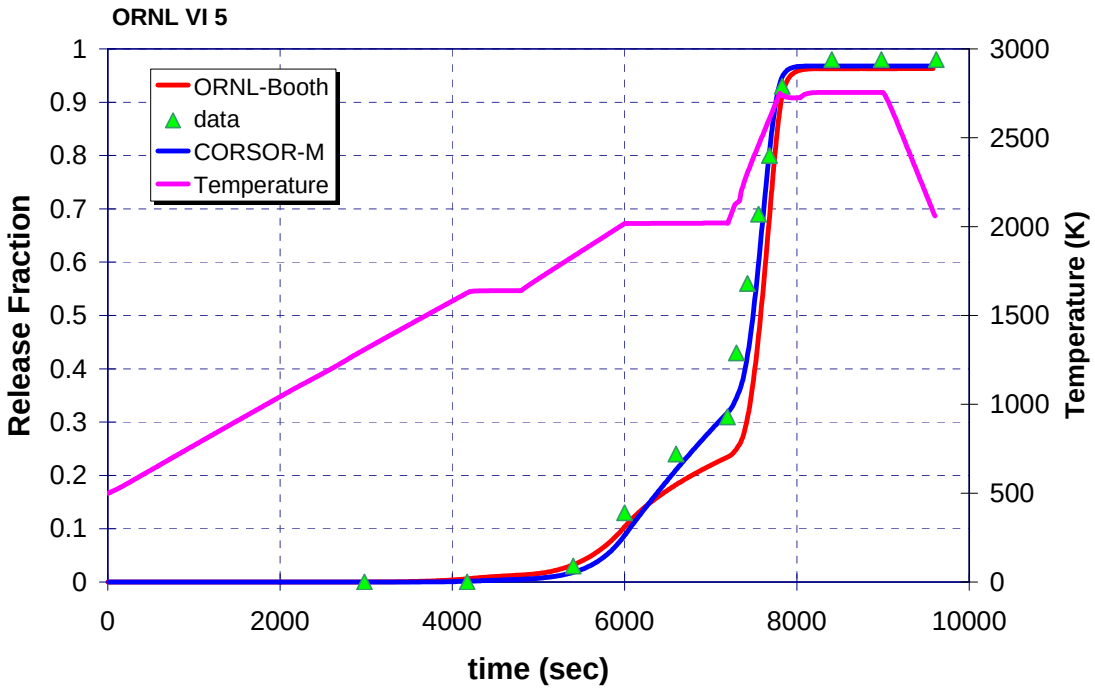

Figure 24. Comparison of Cs release for ORNL Booth modified with CORSOR-M for VI-5 performed under reducing conditions.

Table 3. Total release from ORNL VI-2.

	Experiment	CORSOR-M	ORNL-Booth
Kr	*	.98	.92
Cs	.67	.98	.92
Ba	.18	.003	0.002
Sr		.003	0.002
I	.4	.98	.81
Te		.97	.81
Ru		1×10^{-7}	0.006
Mo	.86	.06	0.42
Ce		1×10^{-8}	1.1×10^{-7}
Eu		1×10^{-5}	1.1×10^{-7}
U	.003	1×10^{-5}	0.001
Sb	.68	0.04	0.93

Table 4. Total release from ORNL VI-3.

	Experiment	CORSOR-M	ORNL-Booth
Kr	1	1	1
Cs	1	1	1
Ba	.3	.04	0.004
Sr	.03	.04	0.004
I	.8	1	1
Te	.99	1	0.99
Ru	.05	10^{-5}	0.03
Mo	.77	0.15	0.88
Ce	0	2×10^{-6}	4×10^{-7}
Eu	0	0.0005	4×10^{-7}
U	0	0.0005	0.003
Sb	.99	0.2	0.93

Table 5. Total release from ORNL VI-5.

	Experiment	CORSOR-M	ORNL-Booth
Kr	1	.97	.96
Cs	1	.97	.96
Ba	.76	.04	0.005
Sr	.34	.04	0.005
I	.7	.97	.96
Te	.82	.95	0.96
Ru	0	10^{-5}	0.03
Mo	.02	0.11	0.85
Ce	.02	3×10^{-6}	4×10^{-7}
Eu	.57	0.0008	4×10^{-7}
U	0	0.0008	0.003
Sb	.18	0.19	0.89

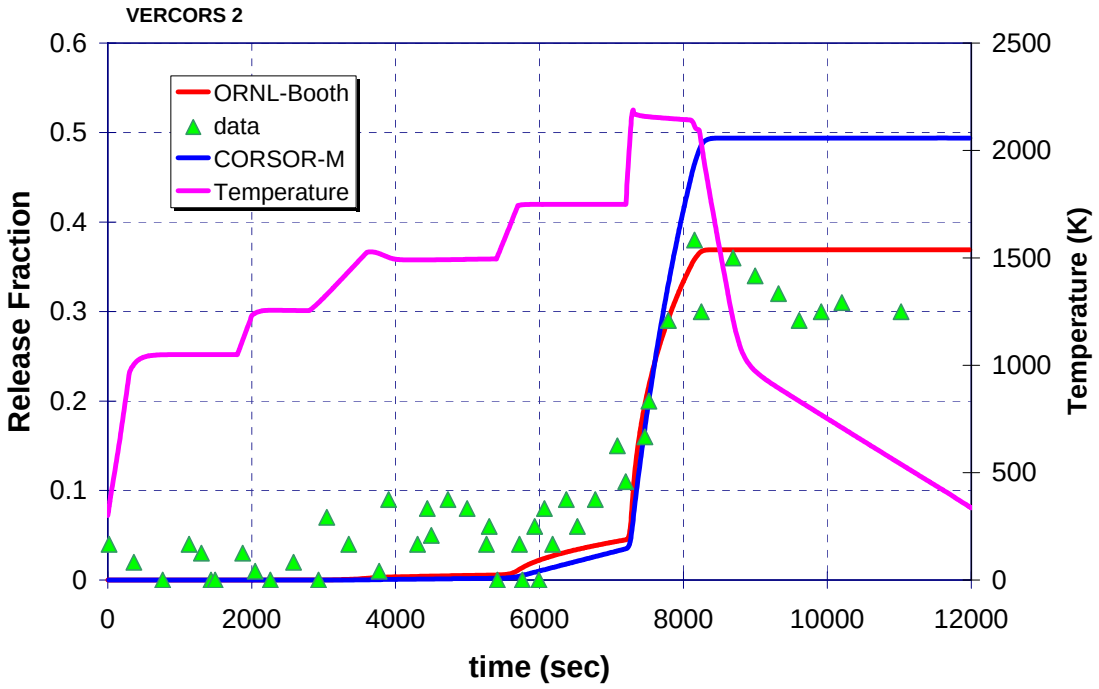

Figure 25. Comparison of Cs release for ORNL Booth modified with CORSOR-M for VERCORS-2.

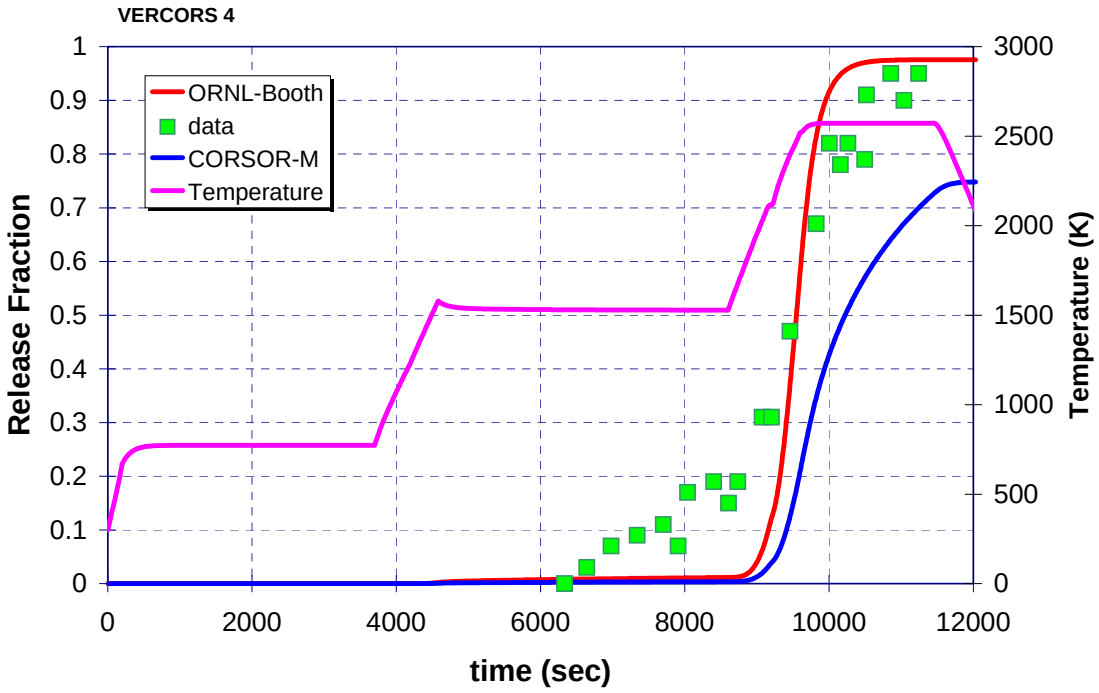

Figure 26. Comparison of Cs release for ORNL Booth modified with CORSOR-M for VERCORS-4.

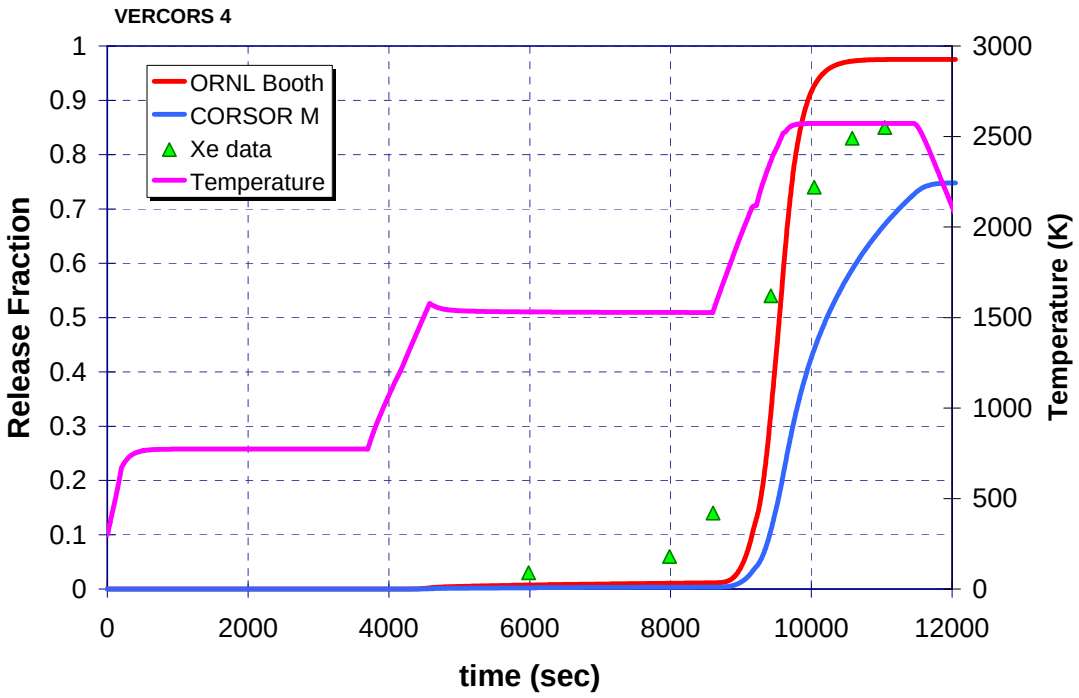

Figure 27. Comparison of Xe release for ORNL Booth modified with CORSOR-M for VERCORS-4.

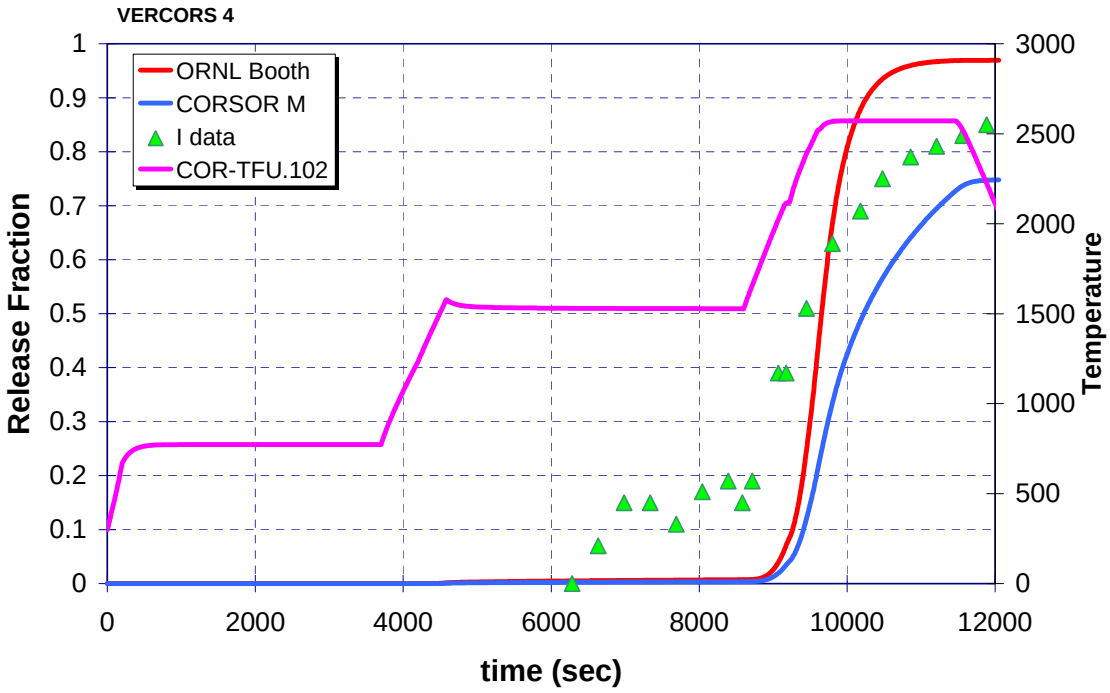

Figure 28. Comparison of iodine release for ORNL Booth modified with CORSOR-M for VERCORS-4.

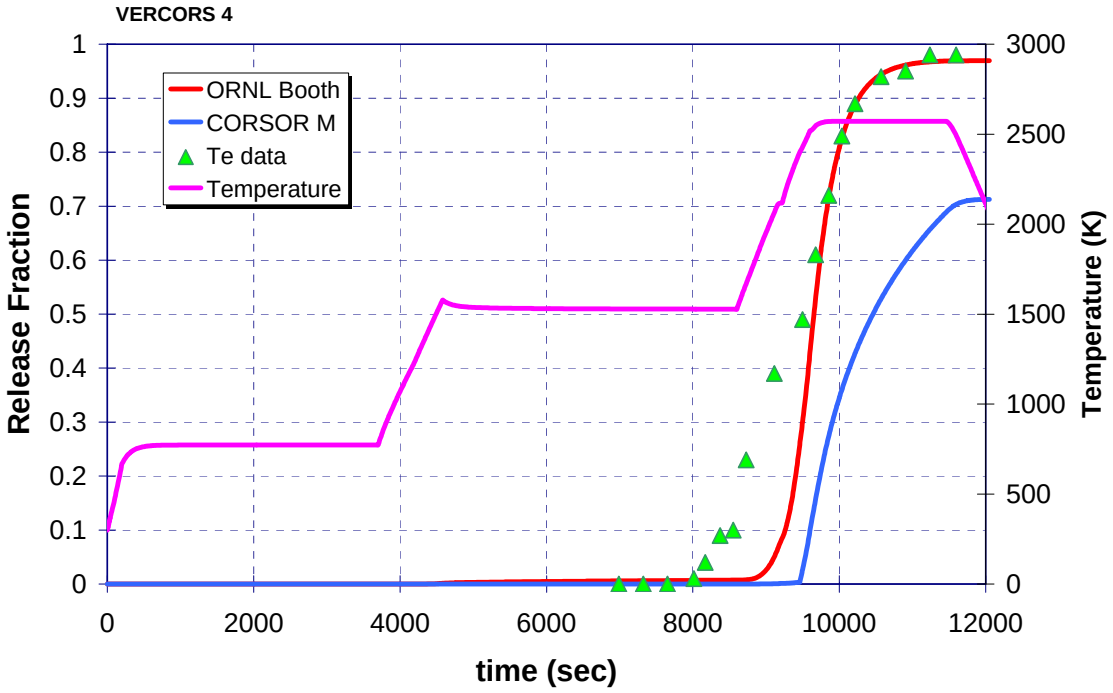

Figure 29. Comparison of Te release for ORNL Booth modified with CORSOR-M for VERCORS-4.

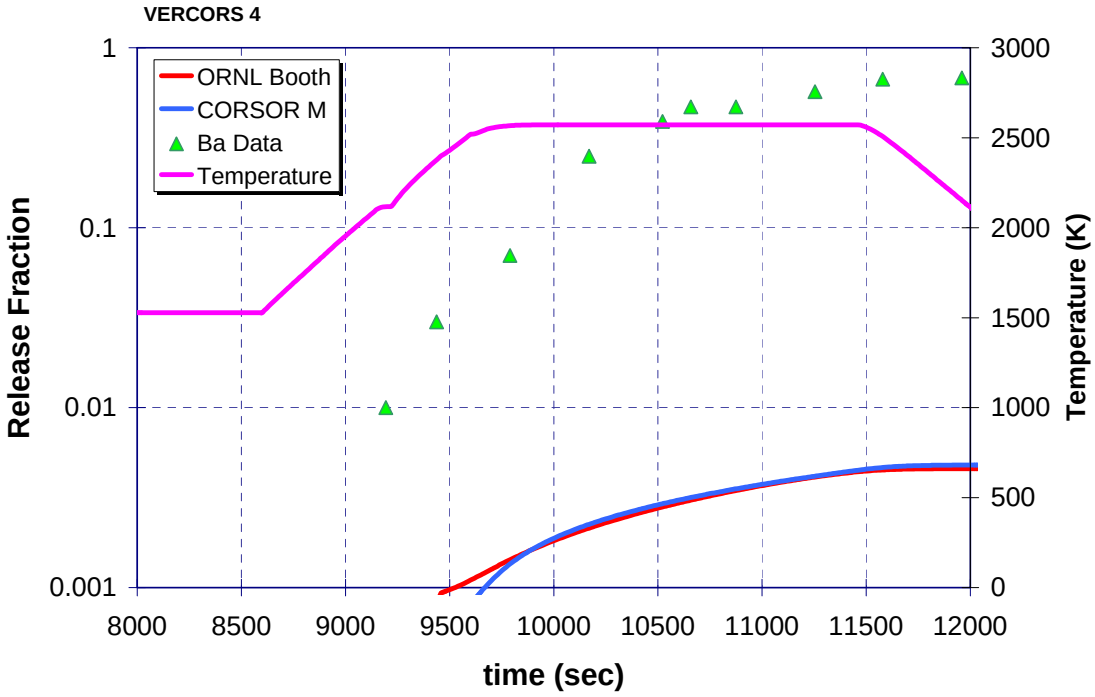

Figure 30. Comparison of Ba release for ORNL Booth modified with CORSOR-M for VERCORS-4.

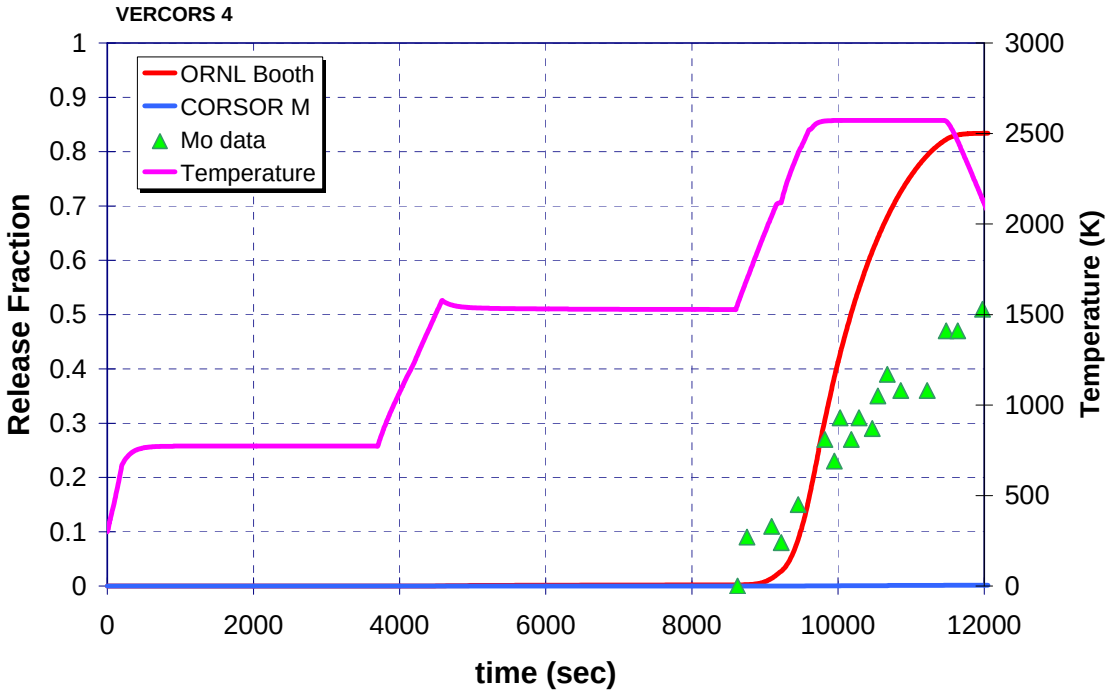

Figure 31. Comparison of Mo release for ORNL Booth modified with CORSOR-M for VERCORS-4.

On balance, the use of the modified ORNL-Booth model produces significantly improved predictions for both the in-pile Phebus FPT-1 test as well as for the small scale ORNL VI and French VERCORS. Barium behavior however remains somewhat problematic. Small-scale tests generally showed greater barium release than is ever observed in the in-piles tests. We believe this is due to more complete oxidation of the zirconium metal cladding on fuel in the small-scale tests, whereas considerably less coherent conditions are encountered in the in-pile integral tests. It is hypothesized that the barium speciation in the small-scale tests is more extensive, leading to higher volatility, than that produced in the in-pile tests where unoxidized Zr is plentiful.

4 Evaluation of Fission Product Deposition Modeling

4.1 Deposition in FPT-1 Circuit (RCS Deposition)

The modified ORNL-Booth release models have been shown to produce favorable release predictions when compared to data from the Phebus FPT-1 test and produce good comparisons with the ORNL VI and French VERCORS tests. The modifications to the vapor pressures for Cs and Mo, which produced favorable release behavior in FPT-1, has an effect on the subsequent deposition of these species in the RCS piping. The effect is illustrated in the Figures 32 and 33.

Figure 32 shows the predicted deposition distribution in the FPT-1 experiment when the default CORSOR-M release model is used. While the total Cs release compares reasonably well with the measured value, and the total Cs transported to the containment is about right, the distribution of Cs deposits in the heated test section above the fuel (upper plenum) and in the steam generator tube do not compare at all well with the data obtained in the test. Deposits in the steam generator are overpredicted and deposits in the heated plenum above the fueled region are underpredicted. In fact, deposits of Cs in the plenum were never predicted to be more than than 0.1% of the initial bundle inventory. What material is predicted to deposit is also predicted to be completely revaporized before the end of the test. Underpredicting deposition in the hot plenum region is a big factor in the over-predicting of the steam generator tube deposits.

Figure 33 shows the Cs distribution predicted for FPT-1 when the modified ORNL-Booth model is used. The lower vapor pressure of the presumed Cs_2MoO_4 results in Cs predicted to be in aerosol form in the hot upper plenum region. As a result, Cs is predicted to be deposited in the upper plenum where it remains for the duration of the test. This, together with a slightly lower total Cs release, results in half as much predicted to be deposited in the steam generator tube, considerably closer to the observed tube deposition. The amount reaching the containment remains about the same, which from a “release to the environment” point of view, one can observe that either model retains about the right amount of fission product within the simulated RCS. The changes in Cs deposition within the RCS could, of course, alter the decay heat distributions throughout the RCS, which in turn could affect revolatilization of other more volatile deposited species, such as CsI, which is transported in addition to the presumed dominant species Cs_2MoO_4.

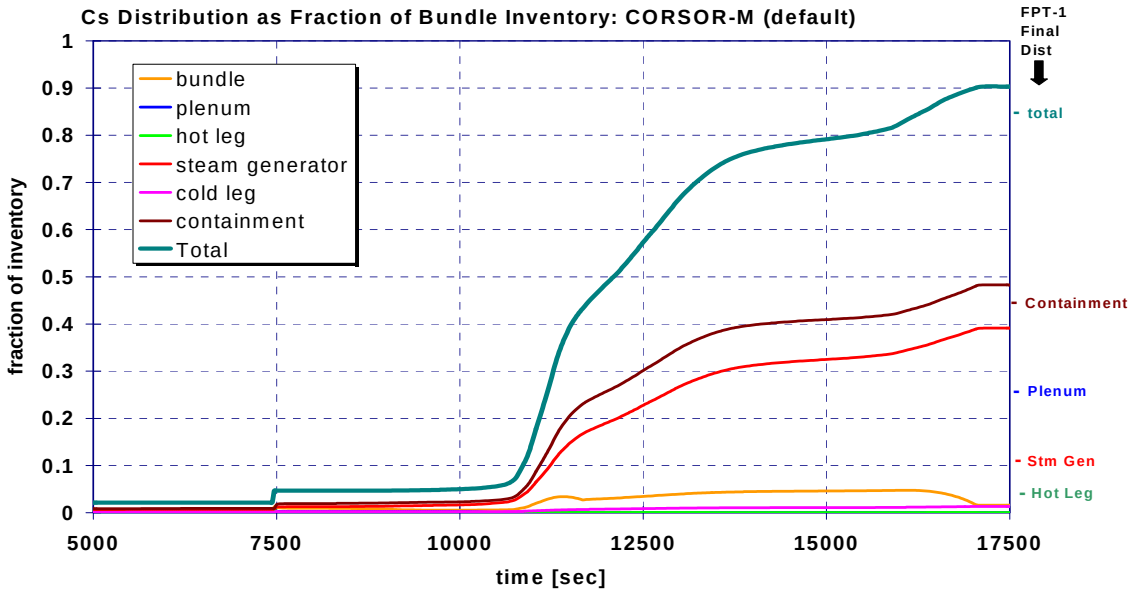

Figure 32. MELCOR-predicted fission product deposition in FPT-1 circuit using default CORSOR-M release modeling. *Predicted plenum deposits for this case were less than 0.1%, not visible on this scale, and were subsequently revaporized.*

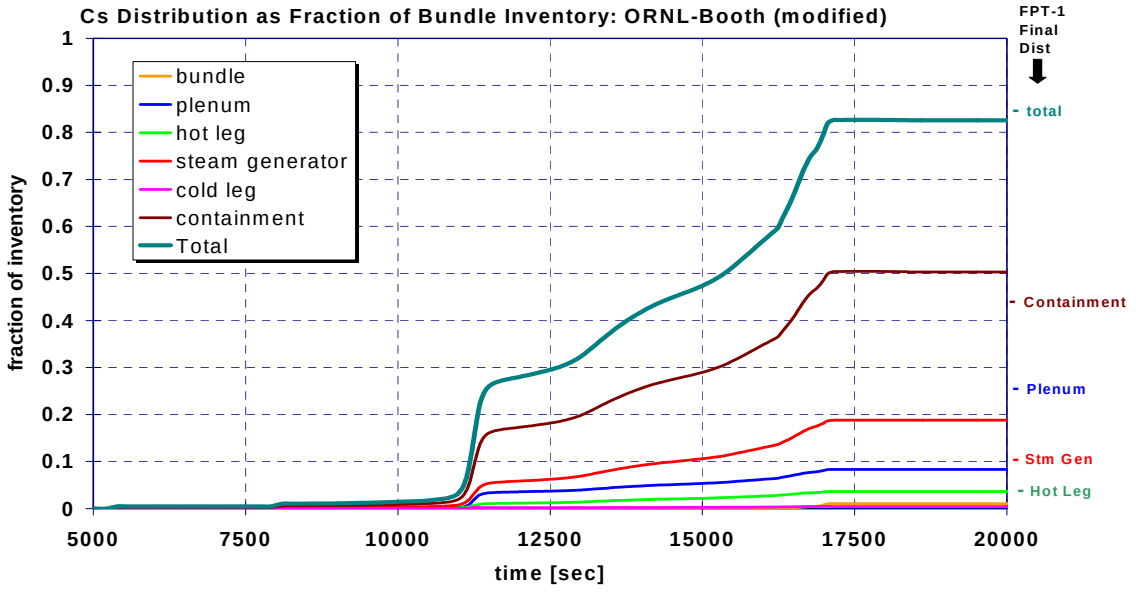

Figure 33. MELCOR-predicted fission product deposition in FPT-1 circuit using modified ORNL-Booth release modeling.

4.2 Deposition within the Phebus Containment

For completeness, the deposition behavior calculated for the FPT-1 containment model is shown in Figures 34 and 35. Shown in Figure 34 is the total airborne aerosol mass in containment predicted using the sources calculated using the ORNL-Booth release model and MELCOR transport models. The suspended mass is normalized to the peak value in order to make comparison to the measured data. This normalization was made necessary because of difference between the magnitude of mass predicted to be transported to the containment, and the measured value. MELCOR predicted only about half of the suspended total mass that was measured. The discrepancy is due to MELCOR's lack of a Ag release model for the Ag/In/Cd control rods and the lack of a model to predict rhenium release from the experiment thermocouples.

The overall depletion prior to the peak airborne value compares quite well. After reaching the maximum value, however, the suspended aerosol mass is predicted by the MELCOR code to deplete less rapidly than was actually observed. This is apparently due to MELCOR underpredicting the particle size as shown in Figure 35, and consequently underpredicting the gravitational settling component of containment deposition. Certainly the underprediction of the suspended mass by a factor of two also resulted in lower aerosol number concentration, perhaps significantly so if the mass is missing from the smaller particle size range, and this may in turn have resulted in slower particle agglomeration and therefore smaller agglomerated particle sizes. If so, this could explain the lower aerosol depletion rate by gravitational settling.

Diffusiophoresis is the other dominant form of aerosol deposition in the FPT-1 containment, and may also be underpredicted, however test data do not provide resolution in this respect. Underprediction of the containment depletion rate errs on the conservative side since more fission products remain suspended in this analysis that might be available for release to the environment. We are presently considering potential treatments for predicting Ag release in MELCOR, however this treatment was not available for these analyses.

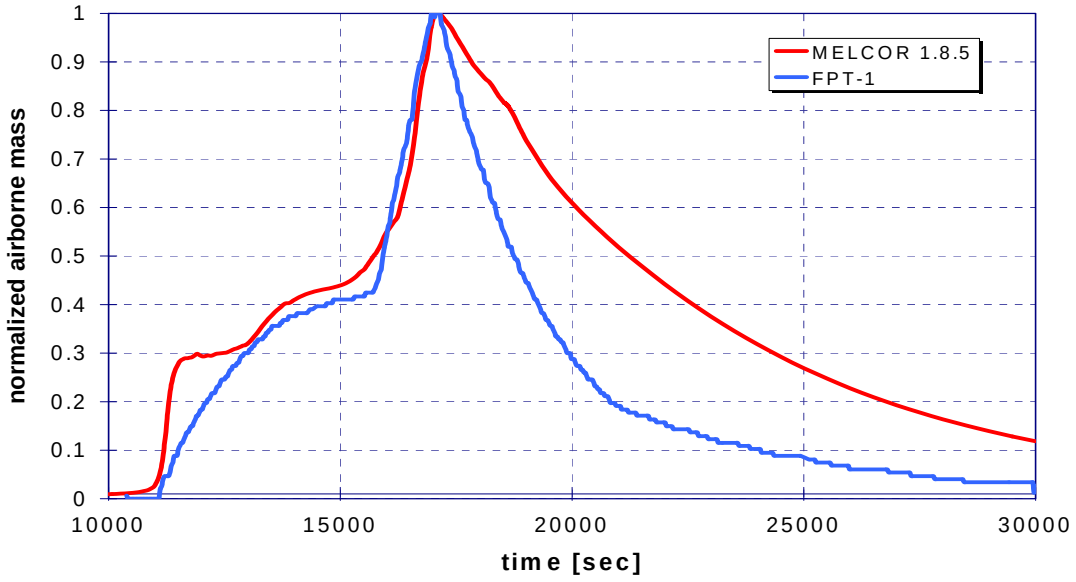

Figure 34. Normalized aerosol depletion rate of airborne aerosol in FPT-1 containment. *The underprediction of particle size and gravitational settling may be the reason for the low predicted depletion rate.*

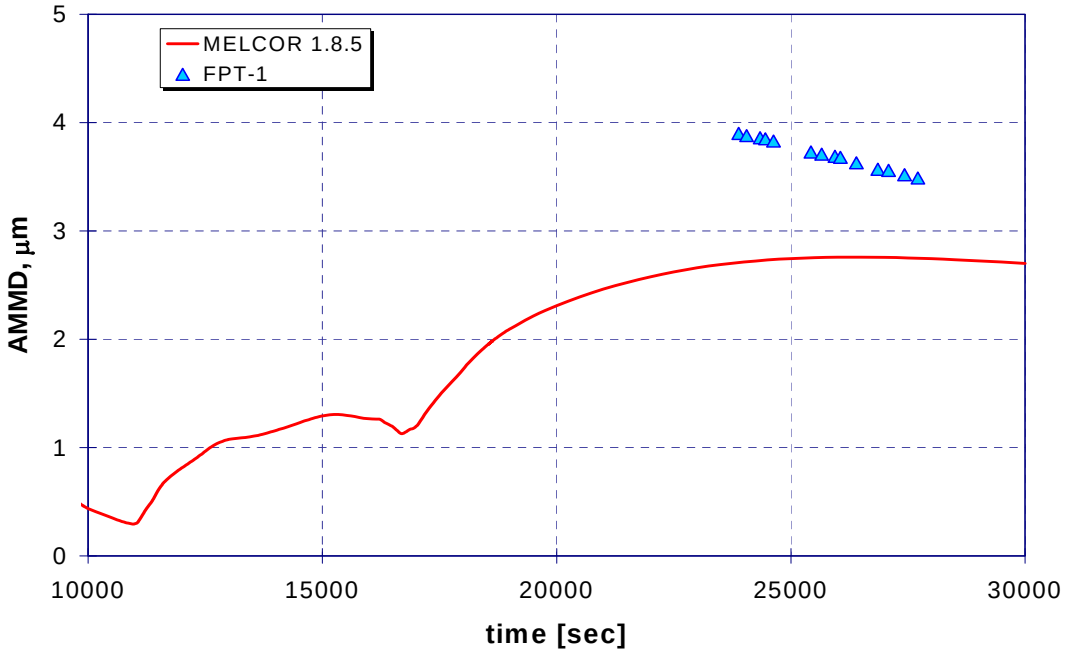

Figure 35. Predicted and measured aerodynamic mass mean aerosol diameter in FPT-1 containment. *Underprediction of the agglomeration rate from too-low airborne total mass may be responsible for the underprediction of the mean particle size.*

5 Estimation of Ruthenium Release under Air-Oxidizing Conditions

The following describes a means of estimating of the ruthenium that may be released from reactor fuel that is overheating while exposed to air. The MELCOR code is used to estimate ruthenium release using the modified ORNL-Booth release model, accounting for mass-transfer limits associated with the vapor pressure of the various ruthenium compounds. MELCOR release models include both a diffusion term for transport in the fuel grain as well as a mass transfer term that limits release according to the vapor pressure of the compound. The mass transfer limiting term in the overall release can considerably affect materials of low volatility.

The default MELCOR implementation of radionuclide class vapor pressure for the case of ruthenium is the lowest of vapor pressures of all MELCOR radionuclide classes, with Mo being a close second in this regard. Both are experimentally observed to be considerably more volatile in view of results from Phebus experiments and VERCORS tests run under steam conditions, which are not as oxidizing as air-conditions.

In order to estimate the increased release of ruthenium when hot fuel is exposed to air, some additional adjustments to the ORNL-Booth release model were made beyond those described in the previous section to account for the greater volatility of ruthenium oxides. Powers *et al.* [13] provide some indications concerning the volatility of RuO_2, as shown in Figure 36. From this figure, it is noted that at 2200K for a moderately hyper-stoichiometric $UO_{2.15}$, the vapor pressure of RuO_2 is approximately 10^{-3} atm, many orders of magnitude higher than the default vapor pressure encoded in MELCOR for the metallic form. Here it is assumed that some fuel oxidation in air leads to this amount of hyperstoichiometry. The low default vapor pressure of Ru in MELCOR prevents prediction of large releases because of the significant mass transport limitation presented by the low vapor pressure. In this estimate, the default Ru vapor pressure was simply scaled to produce approximately 10^{-3} atm at 2200K while retaining the temperature dependence of the metal in order to investigate the effect of a significantly reduced mass transport limitation on the Ru release. The RuO_2 vapor pressure as a function of temperature used in the MELCOR analyses for Ru is shown in Figure 37 along with that of Ru and UO_2 for comparison.

The effect of the increased RuO_2 vapor pressure on predicted release for an analysis of uncovered reactor fuel in a spent fuel pool exposed to air is shown in Figure 38. Also shown in this figure are predicted releases for the default CORSOR-M model and the modified ORNL-Booth model recommend for in-vessel release described in the previous sections. As can be seen, the CORSOR-M release model predicts almost no Ru release, whereas both ORNL-Booth release models predict moderate to significant releases. Where the in-vessel release model has a basis in test measurements under steam oxidizing conditions, it must be emphasized that the estimate for air oxidizing conditions is based solely on the rationale that volatility of RuO_2 dominates the release rate. This assertion certainly bears further evaluation, and future Phebus experiments

are expected to produce data in this area. For the time being, this proposed model can be used to produce estimates for Ru release under air oxidizing conditions that are believed likely to be conservative. An improved provisional model would make use of a fuel oxidation model to predict UO_2 stoichiometry that would work with thermodynamic calculations to predict RuO_2 vapor pressures over the UO_2.

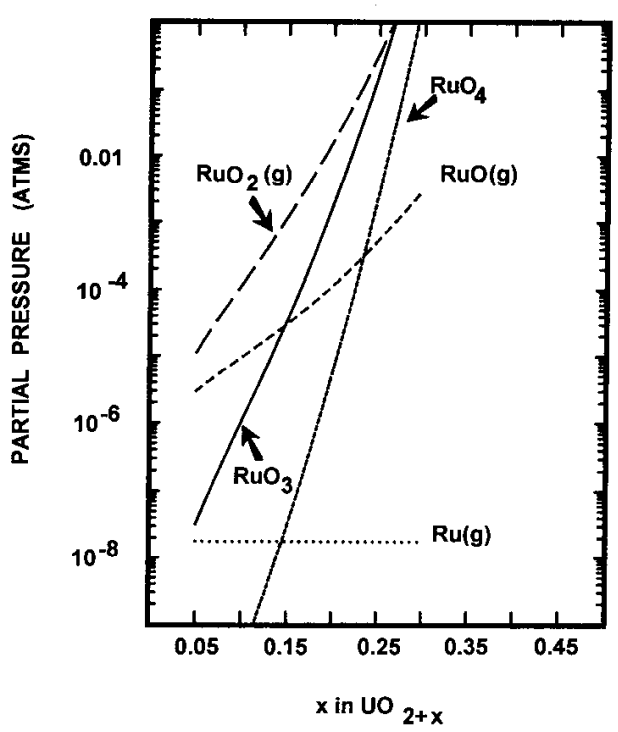

Figure 36. Vapor pressure of Ruthenium oxides over UO_2 at 2200K (NUREG/CR-6218).

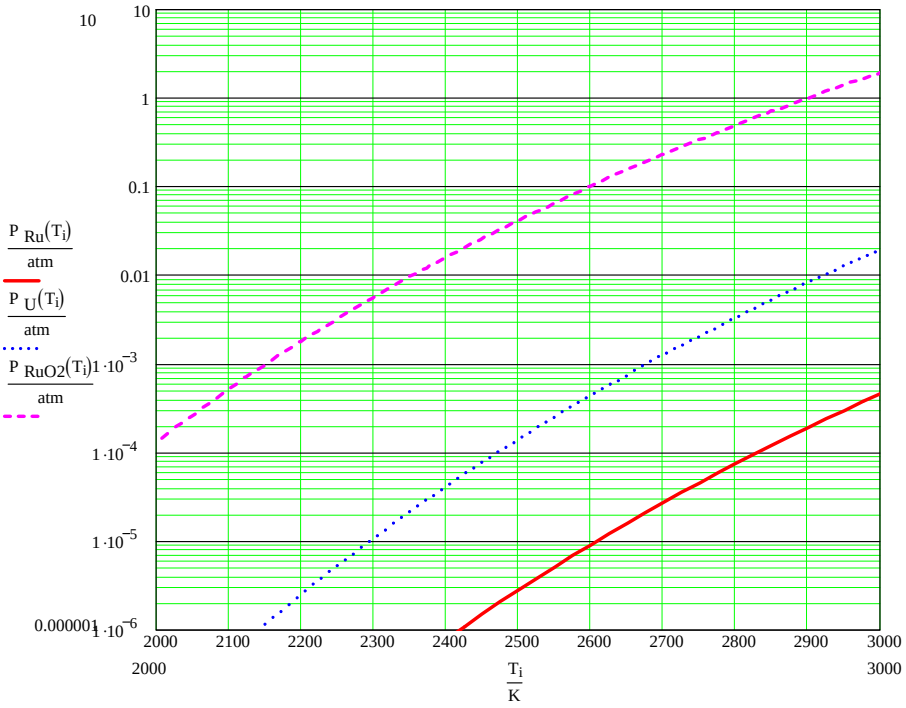

Figure 37. Vapor pressure (atm) of Ru and RuO_2 over $UO_{2.15}$.

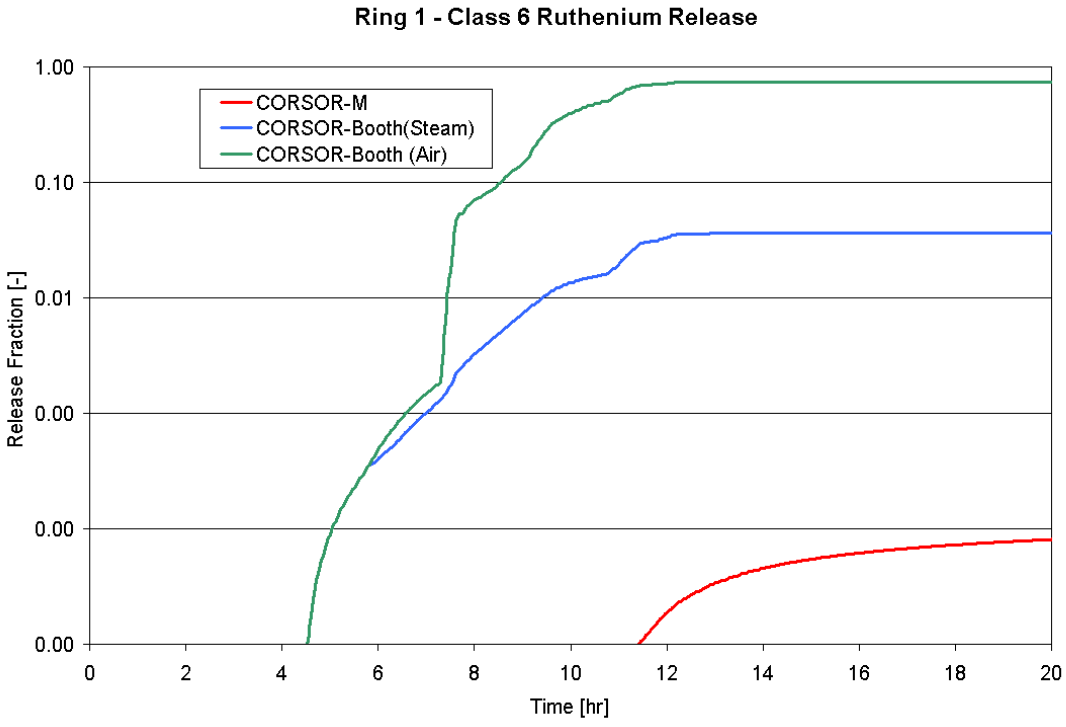

Figure 38. Estimated Ru release for SFP assemblies using ORNL-Booth factors under air oxidation conditions compared to model based on steam oxidation and to CORSOR-M.

6 Zircaloy Oxidation in Air

Accidents occurring in spent fuel pools where air may be available for oxidation with overheated zircaloy fuel cladding require special treatment beyond that available in the default MELCOR 1.8.5 code settings. While provision exists in the default code for predicting oxidation of zircaloy in air, the default air oxidation model is valid only for high temperatures above 1000K. In spent fuel pool accidents, air oxidation can initiate at temperatures as low as 700K, producing sufficient chemical heat that thermal feedback can result in a temperature transient that produces severe fuel damage and fission product release. Oxidation in air produces more chemical energy per mole of reacted zircaloy than oxidation is steam since less dissociation energy is invested than in the case of breaking H_2O into H_2 and O_2 for steam oxidation. Additionally, oxidation in air (oxygen and nitrogen) proceeds more rapidly than in pure oxygen because of differences in oxide scale morphology caused by a simultaneous nitride reaction. The reaction rates for air oxidation are also described by parabolic kinetics similar to the ones used to describe steam oxidation. The general form is

$$\frac{dw^2}{dt} = K(T) \qquad \text{Eq. 11}$$

where *w* is oxide scale thickness or, alternatively, in the MELCOR convention, reacted metal mass. The correlations available to MELCOR for air oxidation are shown in Figure 39. This figure shows the previously recommended correlation for air oxidation in the blue curve. Note that the rate increases between 1200K and 1500K. Recently, Argonne National Laboratory has produced new data on air oxidation, which are shown in the red curve [13]. Present recommendations are to incorporate the new ANL data for the low temperature oxidation temperature range. The rate constant recommended by ANL is

$$K(T) = 3.4311 \cdot \exp\left(-\frac{17258K}{T}\right) \quad \left[\frac{kg^2}{m^4 \cdot s}\right] \qquad \text{Eq.12}$$

where the units refer to the mass of oxide formed.

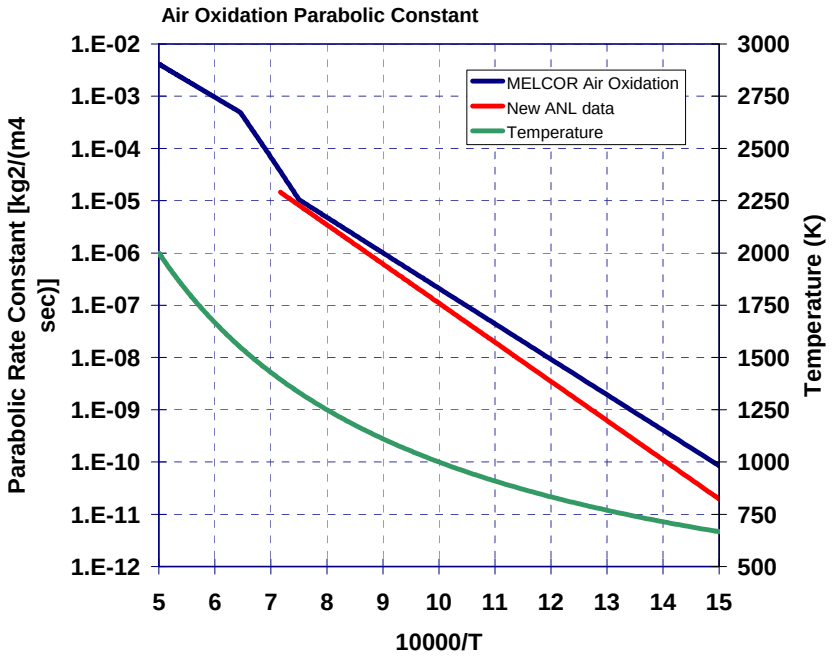

Figure 39. Parabolic reaction kinetics for Zr-air oxidation used in MELCOR.

7 Treatment of Fire and Smoke

Under certain circumstances fire and smoke may be present when fission products are being released. Detailed fire analyses of jet fuel fires can be performed using codes such as VULCAN, which can provide overall guidance concerning rate of combustion and smoke production rate. In order to include the effects of fire in a MELCOR source term analysis, we intend to make use of VULCAN calculation results to prepare MELCOR control functions which will consider the amount of liquid fuel present and given a VULCAN predicted combustion rate, will source into appropriate the volumes energy in the form of radiant energy to the walls, ceilings and floors and sensible energy to the gas in the volume. VULCAN analyses suggest that 20% of the fire energy should be radiated directly to the heat structure surfaces; this will be accomplished using MELCOR tabular functions to introduce heat directly into heat structure surfaces. The remaining 80% of the fire energy will be sourced into the MELCOR CVH gas volume.

An initial fireball is expected to produce a pressure pulse within the building that will open various doors and blowout panels. Separate MELCOR analyses are used to evaluate this short duration event in order to determine appropriate state of doors (i.e. flow paths).

Smoke could potentially affect aerosol agglomeration; however, the properties of smoke particles are highly uncertain.

8 Summary and Recommendations

Based on recent assessments of MELCOR 1.8.5 fission product release modeling against the Phebus FPT-1 test and on observations from the ISP-46 exercise [10], modifications to the default MELCOR 1.8.5 release models are recommended[1]. The assessments identified an alternative set of Booth diffusion parameters recommended by ORNL (ORNL-Booth) [11], which produced significantly improved release predictions for cesium and other fission product groups. Some adjustments to the scaling factors in the ORNL-Booth model were made for selected fission product groups, including UO_2, Mo and Ru in order to obtain better comparisons with the FPT-1 data. The adjusted model, referred to as "Modified ORNL-Booth," was subsequently compared to original ORNL VI fission product release experiments and to more recently performed French VERCORS tests, and the comparisons was as favorable or better than the original CORSOR-M MELCOR default release model. These modified ORNL-Booth parameters, input to MELCOR 1.8.5 as "sensitivity coefficients" (i.e. user input that over-rides the code defaults) are recommended for the interim period until improved release models can be implemented into MELCOR.

For the case of ruthenium release in air-oxidizing conditions, some additional modifications to the Ru class vapor pressure are recommended based on estimates of the RuO_2 vapor pressure over mildly hyperstoichiometric UO_2. The increased vapor pressure for this class significantly increases the net transport of Ru from the fuel to the gas stream. A formal model is needed.

Deposition patterns in the Phebus FPT-1 circuit were also significantly improved by using the modified ORNL-Booth parameters, where retention of lower volatile Cs_2MoO_4 is now predicted in the heated exit regions of the FPT-1 test, bringing down depositions in the FPT-1 steam generator tube to be in closer alignment with the experimental data. This improvement in "RCS" deposition behavior preserves the overall correct release of cesium to the containment that was observed even with the default CORSOR-M model. Not correctly treated however is the release and transport of Ag to the FPT-1 containment. A model for Ag release from control rods is presently not available in MELCOR. Lack of this model is thought to be responsible for the underprediction by a factor of two of the total aerosol mass to the FPT-1 containment. It is suggested that this underprediction of airborne mass led to an underprediction of the aerosol agglomeration rate. Underprediction of the agglomeration rate leads to low

[1] [1] **Note added to proof**: Refined versions of the release models have been incorporated into the 1.8.6 and 2.1 versions of the MELCOR code. Also, a model of silver release from degrading silver-indium-cadmium control rods has been added.

predictions of the aerosol particle size in comparison to experimentally measured ones. Small particle size leads low predictions of the gravitational settling rate relative to the experimental data. This error, however, is a conservative one in that too-low settling rate would result in a larger source term to the environment. Implementation of an interim Ag release model is currently under study.

In the course of this assessment, a review of MELCOR release models was performed and led to the identification of several areas for future improvements to MELCOR. These include upgrading the Booth release model to account for changes in local oxidizing/reducing conditions and including a fuel oxidation model to accommodate effects of fuel stoichiometry. Models such as implemented in the French ELSA code and described by Lewis [4,5] are considered appropriate for MELCOR. A model for ruthenium release under air oxidizing conditions is also needed and should be included as part of a fuel oxidation model since fuel stoichiometry is a fundamental parameter in determining the vapor pressure of ruthenium oxides over the fuel. There is also a need to expand the MELCOR architecture for tracking fission product classes to allow for more speciation of fission products. An example is the formation of CsI and Cs_2MoO_4 and potentially CsOH if all Mo is combined with Cs such that excess Cs exists in the fuel. Presently, MELCOR can track only one class combination (CsI) accurately, where excess Cs is assumed to be CsOH. Our recommended interim modifications map the CsOH (MELCOR Radionuclide Class 2) and Mo (Class 7) vapor pressure properties to Cs_2MoO_4, which approximates the desired formal class combination of Cs and Mo. Other extensions to handle properly iodine speciation from pool/gas chemistry are also needed.

9 References

1. Ramamurthi, M., and M. R. Kuhlman, “Final Report on Refinement of CORSOR – An Empirical In-Vessel Fission Product Release Model,” Battelle Report, October 31, 1990.

2. S.R. Greene, “MELCOR 1.8.2 assessment: comparison of fuel fission product release models to ORNL VI fission product release experiments,” ORNL/NRC/LTR-94/34 (1995).

3. T. Nakamura and R. A. Lorenz, “A Study of Cesium and Krypton Releases Observed in HI and VI Tests Using a Booth Diffusion Model,” Oak Ridge National Laboratory Research Paper (May 1987).

4. B.J. Lewis, *et al*., “Modelling the release behavior of cesium during severe fuel degradation,” J. Nucl. Mater. (227), pp83-109, (1995).

5. F.C. Iglesias, *et al*., “Fission product release mechanisms during reactor accident conditions,” J. Nucl. Mater. (270) pp 21-38, (1999).

6. H. Manenc, P. Mason and M.P. Kissane, “The modeling of fuel volatilization in accident conditions,” J. Nucl. Mater. (294) pp 64-68 (2001).

7. B.V. Dobrov, *et al*., “Kinetics of UO_2 oxidation in steam atmosphere,” J. Nucl. Mater. (255) pp 59-66 (1998).

8. N.E. Bixler, “VICTORIA 2.0: A Mechanistic Model for Radionuclide Behavior in a Nuclear Reactor Coolant System Under Severe Accident Conditions,”NUREG/CR-6131, SAND93-2310 (1998).

9. V. Strizov, “MELCOR 1.8.5 Validation: Modeling of Fission Product Release,” NSI-SARR-149-03, Russian Academy of Sciences, Nuclear Safety Institute, Dec 2002.

10. B. Clement and T. Haste, “Comparison report on International Standard Problem ISP-46 (Phebus FPT-1),” Note Technique SEMAR 03/021, Draft Final Report, April 2003.

11. R. A. Lorenz and M. F. Osborne, “A Summary of ORNL Fission Product Release Tests with Recommended Release Rates and Diffusion Coefficients,” NUREG/CR-6261, (1995).

12. G. Ducros, *et al*., “Fission product release under severe accident conditions: general presentation of the program and synthesis of VERCORS 1-6 results,” Nuc. Eng. Des. (208) pp 191-203 (2001).

13. K. Natesan and W.K. Soppet, “Air Oxidation Kinetics for Zircaloy-4,” Argonne Letter Report, Dec 2002.

Copy to:

Mr. Richard Lee
RES/DSA/FSTB
U.S. Nuclear Regulatory Commission
MS C3A07M
Washington, DC 20555-0001

Mr. Jay Lee
NRO/DSER/RSAC
U.S. Nuclear Regulatory Commission
MS 7 F27
Washington, DC 20555-0001

Mr. Michael Salay
RES/DSA/FSTB
U.S. Nuclear Regulatory Commission
MS C3A07M
Washington, DC 20555-0001

Mr. Mark Leonard
Dycoda, LLC
267 Los Lentes Rd. NE
Los Lunas, NM 87031-9390

INTERNAL RECIPIENTS

Copy to:

MS-0736 Dana Powers, 06762
MS-0748 Nathan Bixler, 06762
MS-0748 Randy Gauntt, 06762
MS-0748 Larry Humphries, 06762
MS-0748, Joonyub Jun, 06762
MS-0748, Don Kalinich, 06762
MS-0748, Jesse Phillips, 06762
MS-0748, K.C. Wagner, 06762
MS-1348, Scott Ashbaugh, 04240